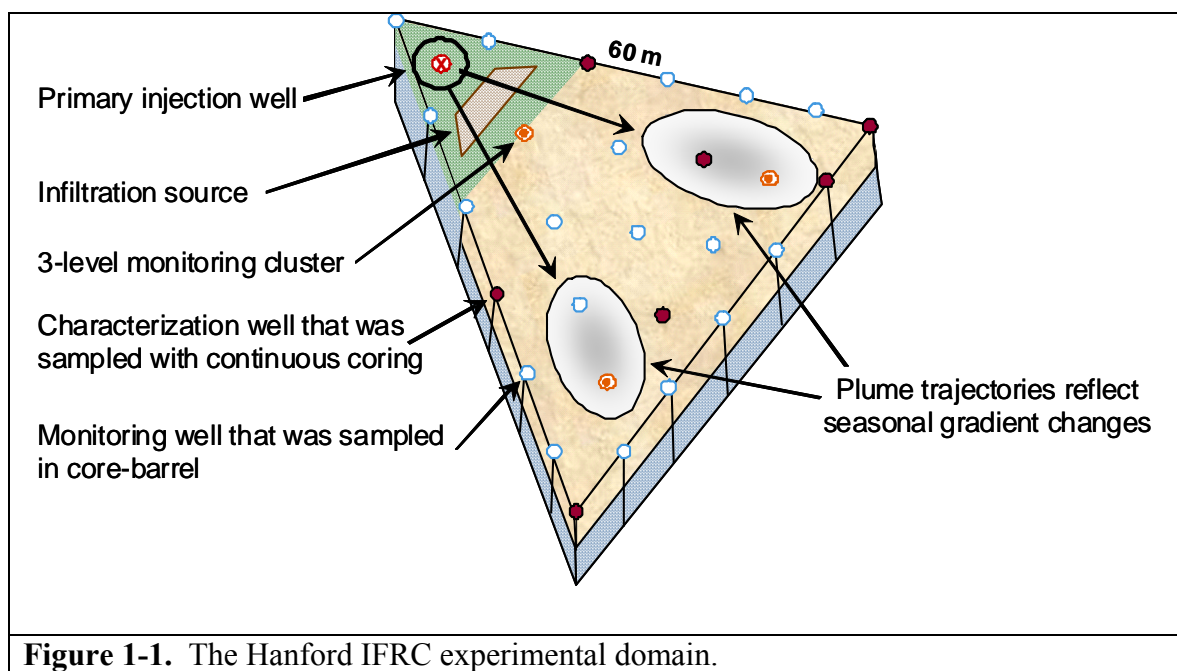


HYDROLOGIC AND GEOCHEMICAL CHARACTERIZATION PLAN FOR THE HANFORD IFRC WELL-FIELD

By the PNNL IFRC Research Team
October 2008

1.0 Introduction and Objectives

The Hanford IFRC project completed the installation of its well-field in August 2008. Photographs from the drilling operation have been posted on the Hanford IFRC web-site (<http://ifchanford.pnl.gov>). The well-field contains 35, approximately 55' (20 m) deep wells configured as shown in **Figure 1-1**. The specifications for the well field and detailed completion plans are described by Bjornstad and Vermeul (2008). Drilling and well completion logs are posted on the website; and a Borehole Drilling, Sampling, and Well Construction Report is nearing completion that will be posted there as well. Twenty six of the wells are open-screened through the entire saturated portion of the Hanford formation, and nine wells are screened over specific depth increments of the saturated portion of the Hanford formation. The well field is to be used for a series of injection and natural gradient experiments to explore mass transfer processes controlling seasonal U(VI) concentrations in groundwater, and factors controlling the activity of the in-situ microbiologic community (see Hanford IFRC web-site). A project research plan is under formulation (IFRC Field Site Experimental Program) that will describe the nature, objectives, scope, and schedule of the different field experiments planned for FY 09-FY 11.



The objective of this project planning document is to describe baseline field and laboratory characterization measurements that will be performed on the completed IFRC well-field and on subsurface samples collected from it. The intent of these characterization measurements is to support development of a robust three-dimensional geostatistical model of the IFRC experimental domain that can be used for reactive transport model development, interpretation of natural gradient field experiments of different types, and properties interpolation of subsurface regions between wells. The methodologies for geostatistical model development will not be addressed in this plan. This document is intended to inform internal IFRC participants, ERSD management, and other ERSD investigators as to the types, methodologies, and numbers of characterization measurements that are currently planned for the IFRC site. Review comments and concerns are solicited. The document will be posted on the Hanford-IFRC website, but will not be released as a formal PNNL report. The plan contents are subject to revision pending accumulated results by various IFRC research participants. It is likely that other characterization measurements will be performed by IFRC participants during the course of their own individual research. Many of those measurements are not captured here, but results, when they are finalized, will be posted to the IFRC database.

A deep characterization borehole was installed along the northeastern margin of the IFRC well-field for microbiologic studies. This borehole successfully sampled sediments of highly variable redox status from the entire unconfined aquifer through the Hanford formation and less-transmissive Ringold Formation. These samples are under active characterization by PNNL Scientific Focus Area (SFA) researchers. The methodologies applied to and results from these measurements and studies will be described through the SFA project.

The organization of this program plan is as follows:

field geophysical measurements, groundwater sampling and composition analyses,

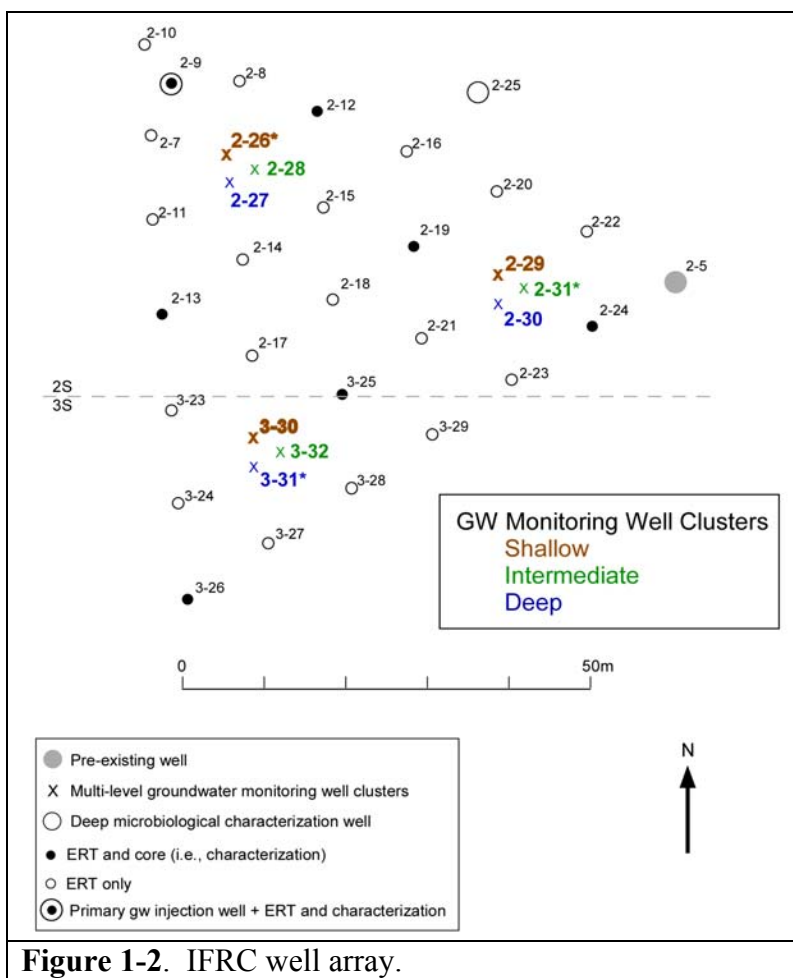


Figure 1-2. IFRC well array.

determination of field hydrologic properties, laboratory characterization of core materials, data integration, and characterization summary.

2.0 Field Geophysical Measurements

Natural sedimentary formations exhibit different geometrical shapes at multiple scales with different structural anisotropy patterns at each scale. The basis of any quantitative stratigraphic model lies in the development of high-quality, multi-scale datasets that can quantify the bed-scale heterogeneity within sedimentary facies. Direct measurement of heterogeneities at the relevant scales using traditional methods has limitations, as many of methods rely on smooth minimum-structure models that ignore fine-scale features within the transmissive units that ultimately control transport behavior. A solution to this problem lies in an improved understanding of the role of heterogeneity in field-scale flow and transport, and the relationship between transport processes and field measurements.

It is known that distribution and geometry of lithofacies exert significant control on the groundwater flow field and the spreading of solutes (e.g., Dagan 1989; Gelhar 1993). In addition to grain-size distributions, lithologic composition and its variation among the different grain-size fractions have been shown to influence the interaction of reactive solutes with sediments (e.g., Weber et al. 1992; Grathwohl and Kleinedam 1995; Ptak and Strobel 1998), to affect structure, and, ultimately, to control the expression of hydrophysical properties of the different lithofacies. Apart from multi-resolution geophysical imaging, the range of methods capable of capturing the detail in subsurface heterogeneity required to better delineate subsurface microenvironments and transition zones is limited.

A primary objective of IFRC characterization is to develop a quantitative 3D model of heterogeneity that accurately reflects variability in primary and secondary sedimentary facies, and the multiscale nature of heterogeneity. The approach combines elements of hydrogeological and geophysical analysis to characterize lithostratigraphy and structure as it controls subsurface flow and transport, and to develop plausible conceptual and predictive hydrogeological models for use at larger scales.

Because all of the geophysical methods require relationships that link fundamental porous media properties (grain size moments, porosity, and permeability) to the geophysical attributes (e.g. seismic velocity, electrical resistivity, and dielectric constant), a secondary objective is to develop robust property transfer models (e.g., petrophysical functions) that represent our understanding of the physical system. The approach seeks to link geological setting and depositional environment to lithostratigraphic properties, and measurable geophysical responses.

Borehole Logging (Temporary Casing)

Just as surface geophysical surveys are used to image the region beneath the surface, borehole geophysical logging provides information about the region beyond the well casing. These logs provide quantitative information on lithology to supplement that derived from visual logging of core and grab samples. Borehole logging will be used to constrain surface geophysical measurements and to derive vertical transition probabilities and length distributions. High-resolution borehole logs will be collected in all 35 wells installed at the IFRC Site. Geophysical logs collected in the temporary casing were limited to neutron thermalization for water content measurement in the vadose zone, and natural gamma spectroscopy to measure natural and man-made γ -emitters over the entire depth interval.

Neutron Thermalization Measurements. Neutron measurements were made with a Campbell Pacific Nuclear (CPN) neutron hydroprobe (Model 503 DR). The probe uses a 50 mCi americium-241 and beryllium source to generate fast neutrons. Fast neutrons collide with the hydrogen atoms in sediment and are slowed down owing to the similarity in the mass of neutrons and hydrogen atoms. The amount of slow neutrons, which is directly related to the amount of hydrogen present, is measured with a helium-3 detector. The main source of hydrogen is associated with water molecules and, therefore, sediment water content.

To measure water content, the sonde is lowered to the top of the water table and the number of neutron counts accumulated over a 16-s interval recorded every 3 inches (0.07 m) while withdrawing the probe from the well. Neutron thermalization theory predicts relatively low count rates in coarse-textured soils (coarse sand and gravel) and relatively high count rates in finer textured soils, such as fine sands, silts, and clays. Thus, in the unsaturated zone, spikes in neutron counts reflect spikes in water content and are generally coincident with fine-textured facies. Conversion of neutron counts to water content will initially be based on existing calibration standards packed with mixtures of siliceous sand and hydrated alumina to mimic water contents of 5, 12, and 20 percent by volume (Engelman et al. 1995). Neutron counts will be correlated with water contents measured on core samples to develop a site-specific calibration.

γ -Ray Spectroscopy Measurements. Borehole γ -ray spectroscopy measurements were made using a spectral gamma logging system (SGLS). The SGLS consists of hardware and software designed to record the distribution of gamma-emitting radionuclides in the subsurface. This system measures spectral and overall natural gamma ray activity from ^{40}K , ^{232}Th , and ^{238}U , which can be used to infer spatial variations in lithology. Most manmade gamma sources emit photons with energies below 1350 keV, i.e. well below the energies of the characteristic photons from natural radioactivity [1461 keV for ^{40}K , 1765 keV for ^{214}Bi (from the uranium decay chain), and 2615 keV for ^{208}Tl (from the thorium decay chain)].

SGLS uses a NaI detector for gross γ -ray measurements, and an 18% relative efficiency high-purity germanium detector for quantitative spectral measurements.

To measure the γ -ray spectra, the sonde is lowered to the bottom of the well and spectra accumulated over a 16-s interval recorded every 6 inches (0.15 m) while withdrawing the probe from the well. A significant part of ^{238}U and ^{232}Th is bound in dark-colored, ferromagnetic and titanium-containing minerals in the sediments (Kogan et al. 1969; Zachara et al. 2007). This implies that the γ -ray activities of sands should be a function of the grain size, density, and heavy mineral content. ^{40}K is uniformly spread throughout the principal rock-forming minerals, such as quartz and feldspar, and sediments with the same parent materials. Thus, soil separates with similar grain sizes even from different locations often display similar ^{40}K activities. A high ^{40}K activity typically results from an elevated fines content arising from K-containing micas and their weathering products, and is indicative of fine-textured subsurface zones. Conversion of γ -ray counts to specific isotopic activities will initially be performed using calibration standards. These standards consist of buried concrete models with known amounts of K, U, and Th (Stromswold, 1994). Relationships between grain size moments, derived from core and grab sample measurements described in Section 5, and γ -ray counts (gross, natural radioactive elements, ^{40}K , ^{238}U , and ^{232}Th , and their ratios) will be developed to allow quantitative descriptions of lithology from down-hole SGLS logging.

Post Completion Well Logging (PVC Wells)

All of the wells were completed in 4-in diameter PVC well casing. The annulus between the smaller PVC casing and the original hole is filled with medium-textured sand in the vadose zone and coarse-textured sand in the saturated zone, with grout in the 0-10 ft backfill interval. All of the vadose zone sensors (thermistors for temperature and vertical electrode arrays for resistivity measurements) were installed in the annulus. The presence of the vadose zone instruments and associated cables in the annulus will limit the types of borehole geophysical measurements that can be made, and will impact data quality, overall, in the vadose zone. Post-completion well logging will be conducted to establish cross correlations between the temporary casing measurements and those in the final well bore that will be used for long-term monitoring. Six different borehole geophysical logs were selected for post-completion logging, including: bulk density, porosity, electrical conductivity, cross-hole radar, acoustic televiewer, and borehole deviation. Bulk density and porosity logs will be collected in collaboration with the USGS Geophysics group (Storrs, CT) whereas the remaining logs will be collected in collaboration with Golder Associates (Tacoma, WA).

Bulk Density. Borehole density logs provide measurements of the depth-dependent bulk density (ρ_b) and the borehole-compensated photoelectric factor (P_e), critical factors for the accurate determination of porosity and lithology. It is assumed that the logging density accurately represents the *in situ* sediment bulk density. The logging density should be similar

to bulk density derived from core measurements, corrected for any elastic rebound experienced by the sediment when it is extracted from the borehole.

Density measurements will be made using the Mount Sopris 2GDA-1000-S density probe. The standard 2GDA-1000-S is a dual-detector tool optimized for use with sources of 100 μCi ^{137}Cs to 75 mCi ^{137}Cs . The source-to-detector offsets are 4 and 11 cm. The probe measures density by irradiating the borehole wall with gamma rays and measuring the flux between the radiation source and the receivers. The probe measures back-scattered radiation in the Compton energy band and includes a photoelectric window and a Compton window so that Z/A ratios can be measured. Returns of low-energy gamma rays are converted to a photoelectric effect, P_e . The P_e depends on electron density and therefore responds to bulk density and lithology. It is particularly sensitive to low-density and high-porosity zones. The thin bed resolution is better than 2 cm. Density measurements will be performed on all the IFRC wells. Bulk and particle densities derived from measurements on grab and core samples will be used to refine calibration of the downhole logging.

Porosity. Neutron porosity measurements are obtained using fast neutrons emitted from a 10 Ci americium oxide–beryllium (AmBe) source. As with water content measurements, the rate at which the neutrons slow down to epithermal and thermal energies is controlled largely by the amount of hydrogen present. The neutron logs are affected by different lithologies because the tool is calibrated for 100% limestone. Neutron porosity logs are processed to eliminate the effects of borehole diameter, tool size, and temperature. Formation fluid salinity, lithology, and other environmental factors also affect neutron porosity. Of particular importance is the presence of chlorine in the PVC casings, which is known to slow down neutrons. These parameters must be estimated for each borehole during neutron log processing.

Porosity measurements will be made with the Mount Sopris 2NUA-1000 Neutron-Thermal-Neutron tool. Data output from the tool includes apparent neutron porosity (i.e., the tool does not distinguish between pore water and lattice-bound water), formation bulk density, and the photoelectric effect. Measurements of porosity derived from undisturbed core samples, actual and logging derived bulk densities, and measurements of particle density will be used to develop 3D maps of porosity for the site.

Electrical Conductivity. Electrical conductivity logs provide information on the change in electrical conductivity of the sediment surrounding the borehole as a function of depth. The electrical conductivity of sediment (and its reciprocal, electrical resistivity) depends on the degree of water saturation (porosity in the saturated zone), pore water conductivity, texture (via surface conductance), and temperature. It is therefore a useful tool for quantifying changes in these properties with depth. When integrated with other borehole logs (e.g., natural gamma logs, lithologic logs, or other geophysical logs) the hydrogeologic factors controlling the conductivity log response can be determined.

Electrical conductivity measurements will be made using a Mount Sopris 2PIA-1000 probe that measures down-hole electrical conductivity and magnetic susceptibility. The 2PIA-1000 probe includes a standard poly probe top that allows use of the induction tool beneath the 2PGA-1000 gross gamma sonde. A small transmitter coil in the sonde creates a primary magnetic field to make the measurement. The magnetic field creates an electric field in the material surrounding the borehole, which in turn, creates electrical "eddy current" flow within the sediment. The strength of the eddy current depends on the electrical conductivity of the material. The eddy currents create a magnetic field, which is detected and measured with a receiver coil in the probe. Within the normal range of operation of the borehole equipment, the quadrature signal (i.e., the signal 90° out of phase with the primary field) is proportional to the conductivity of the material surrounding the borehole. The zone of influence of the induction tool is between 20 cm and 100 cm from the borehole, which should minimize the effects of the backfill materials. The tool has an intercoil spacing of 0.5 m which provides a vertical resolution of around 0.5 m. However, layers as thin as 0.1 m can be detected if there is sufficient conductivity contrast with the adjacent layers.

This tool allows simultaneous measurement of electrical conductivity and magnetic susceptibility as a function of depth through the well casing. The conductivity probe is based on the Geonics EM-39 slim line induction tool and is optimized for conductivity readings. Therefore magnetic susceptibility measurements are somewhat qualitative. Conductivity is measured in mS/m whereas magnetic susceptibility is measured as a percentage of primary magnetic field. Continuous measurements will be made over the entire depth of the well but it is anticipated that vadose zone sensors installed in the annulus of the well casing will render these data difficult to interpret. Electrical conductivity and magnetic susceptibility will also be useful for interpreting density and porosity logs.

Borehole Deviation. Without accurate information on borehole inclination, travel time discrepancies in crosshole radar and seismic measurements may be misinterpreted as an anisotropy effect. Uncertainty in the relative positions between the monitoring and injection wells can also have a cumulative, nonlinear effect on inverted transport parameters. To minimize this source of uncertainty, borehole deviation will be measured on the 35 IFRC wells using the Mount Sopris 2DVA-1000 probe. The probe contains a three-axis magnetometer and a three-axis accelerometer for making measurements which are temperature corrected by a down-hole microprocessor. The probe reports borehole inclination, bearing, true vertical depth, northing, and easting. These parameters are calculated in real time using the quantities measured by the probe.

Acoustic Televiewer. Detailed information on well completion, including the presence of fractures, borehole breakouts, borehole form and stability and the location of thin beds is essential to the accurate interpretation of flow and transport experiments. To determine the quality of well completion and identify the location of any possible voids or unstable regions,

a borehole televiewer will be used to provide acoustic images of the region near the borehole wall.

Measurements will be made using a Mount Sopris FAC40 televiewer. The FAC40 produces images of the borehole wall that are based on the amplitude and time of travel of an ultrasonic beam reflected from the formation wall. The ultrasonic energy wave is generated by a piezoelectric ceramic crystal at a frequency of around 1.4MHz. When triggered, an energy wave is emitted by the transducer and travels through the acoustic head and borehole fluid until it reaches the interface between the borehole fluid and the borehole wall. Here a part of the beam energy is reflected back to the sensor, the remainder continuing on into the soil at a changed velocity. The travel time for the energy wave is the period between transmission of the source energy pulse and the return of the reflected wave measured at the point of maximum wave amplitude. The magnitude of the wave energy is measured in dB, a unit-less ratio of the detected echo wave amplitude divided by the amplitude of the transmitted wave. Vertical resolution depends on logging speed and range from 0.5 in at a logging speed of 450 ft/hr to 3 in at a logging speed of 2600 ft/hr. Horizontal resolution depends on signal frequency, sampling rate, and borehole diameter but in most cases ranges from 0.15 inches to 0.3 inches. Travel time and signal amplitude data are typically displayed as color coded maps with depth and orientation information. Vertical fractures appear as straight lines, while fractures dipping between vertical and horizontal appear as sinusoidal traces.

Neutron Thermalization Measurements. Neutron measurements will also be made after well completion to map water content changes in the vadose zone due to meteoric recharge, water table fluctuations, and groundwater mounds from injection experiments. Measurements will be made using the Campbell Pacific Nuclear (CPN) neutron hydroprobe (Model 503 DR) as previously described. Calibration of the neutron hydroprobe for measurements in the IFRC PVC wells will be accomplished in two steps. An empirical calibration will be developed first by correlating moisture content measurements from the core samples with neutron counts. This calibration will then be refined using Monte Carlo Neutron Photon (MCNP) modeling (Briesmeister 1997). Numerical simulations of neutron transport using multi-group neutron diffusion theory (Li et al. 2003) and Monte-Carlo methods (Mickael 1991; Nyhan et al. 1994) have proven effective for developing calibration functions for these types of conditions (Keller et al. 2005). MCNP simulations will be used to predict the count rate for a neutron probe of known geometry based on sediment bulk density, moisture content, sediment elemental composition, and access tube configuration.

Borehole Radar. Borehole radar is similar to conventional GPR except that boreholes are used to place the antennas relatively close to the regions to be characterized, resulting in more precise imaging. Measurements can be made in a single borehole (single-hole reflection survey) to obtain information from the entire volume of sediment surrounding the hole and to determine the orientation of features like thin beds. The receiver and transmitter

antennas may also be lowered into different holes to allow cross-hole and tomographic measurements. The information obtained with crosshole measurements is complementary to the single-hole reflection surveys. These surveys are used to measure the radar wave velocity and attenuation. The propagation of electromagnetic waves through sediment is primarily a function of the dielectric constant and the electrical conductivity. The potential for a particular feature to be identified is determined by the contrast in the dielectric permittivity of the feature and surrounding sediments.

The immediate post-completion characterization will be based on single off-set borehole surveys in order to make data available to modelers as soon as possible. In this method, the transmitter and receiver are deployed in different holes but at the same depth for each measurement. At a later date, additional surveys including borehole reflection, borehole tomography and borehole to surface measurements will be conducted. Measurements will be made using the RAMAC/Borehole system manufactured by Mala Geoscience. The area of investigation is a cylinder shaped volume around the borehole with a radius of 10-100m (depending on electrical properties of the media). Owing to the relatively homogenous nature of the vadose zone and the presence of sensors in the annulus of the wells, vadose zone data may not of high quality. Thin beds of fine-textured sediments would normally produce strong reflectors, but these may be difficult to deconvolve due to sensors and cables. However, the large contrast in permittivity between dry vadose zone sediments (≈ 5) and the water-filled pores of the saturated zone (permittivity constant for water is 81) should allow clear identification of the water table. Moreover, within the saturated zone, spatial variations in water-filled pores owing to porosity differences should lead to large enough contrasts for detection in cross-hole measurements. The single offset surveys will be performed on all two-well combinations with spacings of 30-ft or less.

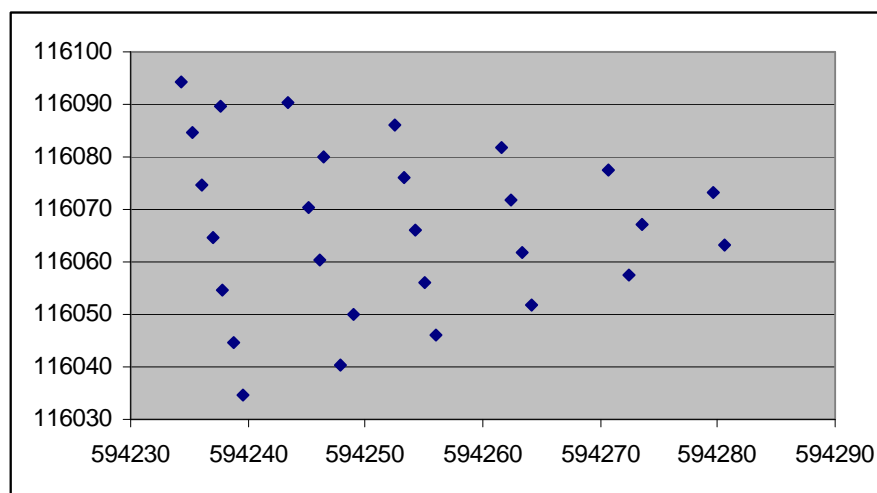
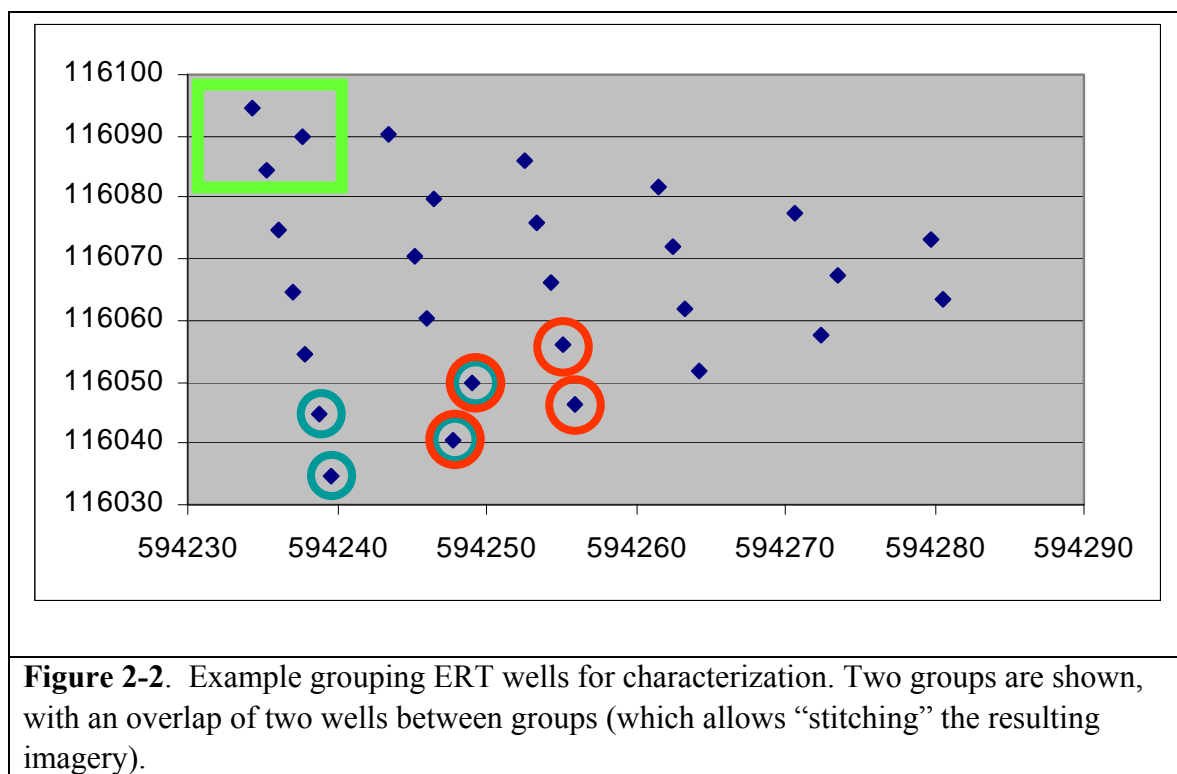


Figure 2-1. Layout of IFRC Well field showing ERT Instrumented wells.

Electrical Resistance Tomography. The initial post-completion resistivity characterization will be performed among the wells using a leapfrog approach. In this approach, subareas of the well field will be characterized using cross-hole resistivity measurements, and the resulting images will be stitched together mathematically. There are 28 instrumented resistivity wells (**Figure 2-1**) with a total of 840 electrode locations. With existing resistivity hardware, it is possible to collect resistivity data from up to four wells at a time. New, more robust instrumentation is being sought through a capital equipment request.

By collecting data from wells in groups of four, there will be an overlap of two wells per set of measurement series (**Figure 2-2**). Thus, with approximately fifteen data collection campaigns, each lasting about 1-2 days, the initial characterization of the field site could be completed. An initial data acquisition optimization effort is currently underway using the northernmost three wells (green box in **Figure 2-2**) to determine the best measurement approach for the leapfrog effort. The optimization study was completed at the end of September 2008, and the full 3D survey is now underway. The 3D survey will be coordinated with field hydrologic characterization (Section 4) because it provides complementary data for the estimation of field-scale hydrologic properties.



Following the initial characterization, data collection will be modified to include interrogation with both surface and borehole electrodes. The modified approach will use two lines of surface electrodes, installed in a N-S and E-W direction to collect surface to borehole

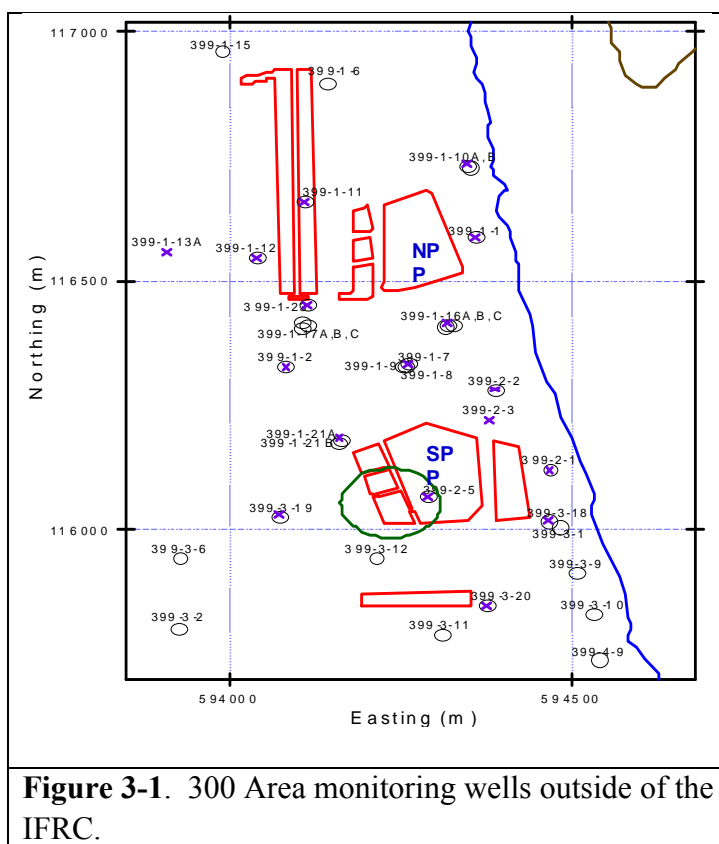
data. As with the leapfrog approach, this configuration will first be evaluated at select locations to determine whether there is any improvement in data quality or resolution. The resulting data will be processed to generate a 3D distribution of electrical resistivity values for the entire well field.

3.0 Groundwater Composition

The objective of baseline characterization of IFRC sediments and groundwater is to provide an estimation of the site's three-dimensional variability in lithology and geochemical properties. The resultant information will be used to formulate detailed hypotheses regarding the geochemical component of reactive transport. Unlike the sediment components, which respond to environmental changes relatively slowly, and whose parametric values are relatively constant, the groundwater phase is rapidly mutable, so characterization requires multiple sampling events over time.

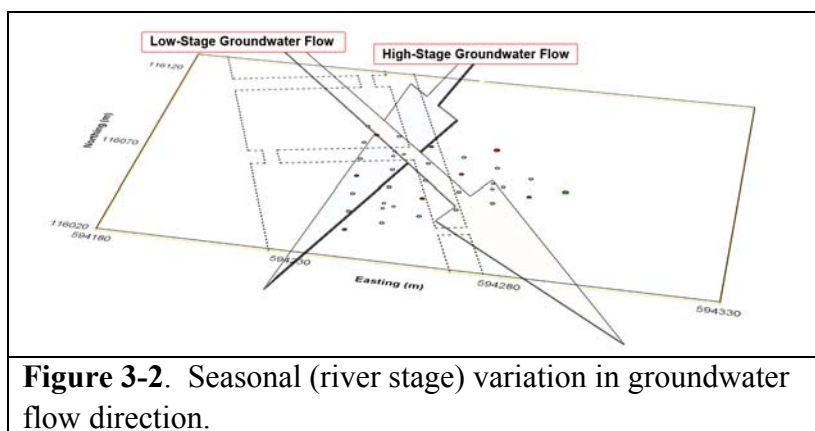
The level of effort for groundwater sampling can be adjusted to suit research goals and circumstances. Initial and repeated assay samplings, for example, can be relatively course in compositional detail. These measurements can then be supplemented by detailed, contextual, hypothesis-driven sampling at specific positions within the aquifer, for specific chemical components. This approach has the benefit of providing a rapid assessment of general geochemical conditions, so that subsequent measurements can be focused on specific questions. The samples at the IFRC will be collected in this manner, with relatively frequent sampling of major groundwater components, and intensive, targeted sampling during subsurface experimentation.

Sampling and analysis was begun in early September, 2008, and consisted of pumped samples from all new IFRC groundwater wells. The sampling and analysis of the IFRC groundwater will include several sampling purposes, and samples will be numbered to provide an



association with purpose. Sampling will be conducted in purpose driven ‘campaigns’, and each campaign will be given a lettered prefix (e.g., BL for Baseline). A sequence number will be assigned for sampling iterations within the campaign. The well-specific numbering scheme will be applied along with this protocol. For example, the first water samples will be assigned numbers such as ‘BL1-3-13’, describing the baseline sample no. 1 from well 399-3-13.

Well construction at the IFRC produced a triangular array (**Figure 1-2**), numbered according to an established convention for the Hanford site. With respect to the ability to sample and characterize groundwater, the well completions were within three categories: i.) a single well (no. 2-25) was completed with screen from near the top of the Ringold formation into the top of the underlying Columbia River Basalt; ii.) all other wells, with the exception of three, three-well clusters, were completed with screens extending through the saturated Hanford formation into the top of the Ringold formation; and iii.) one each of the three, three-well clusters was completed at an upper, middle, or lower isolated depth within the saturated Hanford formation. The absolute depth range of the screen interval was determined by the depth to the top of the Ringold formation and the number of fixed, stock unit-lengths of available screen that could be installed from that depth upward. The screened interval was set to reach upward into the vadose zone, to include the highest annual elevation of the seasonally variable water table. Each well was developed and equipped with a down-hole pump in the middle of the saturated zone, controlled from a central laboratory trailer for automated sampling. Some wells were also equipped with an electrode array capable of continuously monitoring temperature, pH, and bromide; all of the wells will eventually include electrode arrays. Pumps and monitoring equipment is removable for calibration, service, and to accommodate experimentation needs. Samples will be collected as needed, and analytical data will be recorded in the IFRC database.



Baseline groundwater characterization will evaluate hypotheses regarding the seasonal and three-dimensional nature of the site. The IFRC is located within a broader field of contaminated and uncontaminated lands that is penetrated by abundant monitoring wells (**Figure 3-1**), and is hypothesized to include three-dimensional mixing of up-gradient groundwater and down-gradient river water. These components are under the local influence of the changing hydrologic gradient imposed by the rise and fall of the nearby Columbia

River: the proportions of ground and river water change with hydrologic head. In addition, stratigraphic variations could cause short-term heterogeneity across the IFRC in the mixing of ground and river water. The hydrologic gradient experiences short-term (daily and weekly) variations at a relatively small scale and seasonal variations on a grosser scale. Flows are generally to the southwest, from the river, at high water in the Spring, and generally to the southeast, toward the river, at low water in the Fall (**Figure 3-2**). Characterization will therefore progress from bulk characterization as soon as possible (Opportunity Pumped Samples), to seasonal high and low stage sampling of pumped waters (Timed Pump Samples), to multi-level sampling of selected vertical groundwater profiles (Multi-Level Samples), to temporal sampling of variations in samples from within the area near the water table (Smear Zone Samples).

Opportunity Pumped Samples. An automated pumped-sample laboratory is deployed to the IFRC (**Figure 3-3** and Section 4.0), and will collect a set of groundwater samples as soon as practicable. The samples will include all of the IFRC wells, and a set of samples from the surrounding area, including proximate 300 Area monitoring wells (**Figure 3-2**; 399-1-7, 399-2-1, 399-3-18, 399-3-20, and 399-3-12) that may be used as water sources for hydrologic testing or injection. The sampling system consists of remotely controlled down-hole pumps, which can be consecutively activated to deliver water to the site laboratory. A flow cell is equipped to monitor pH, conductivity, and turbidity, and when these parameters show constant values groundwater is sampled into clean containers of choice.

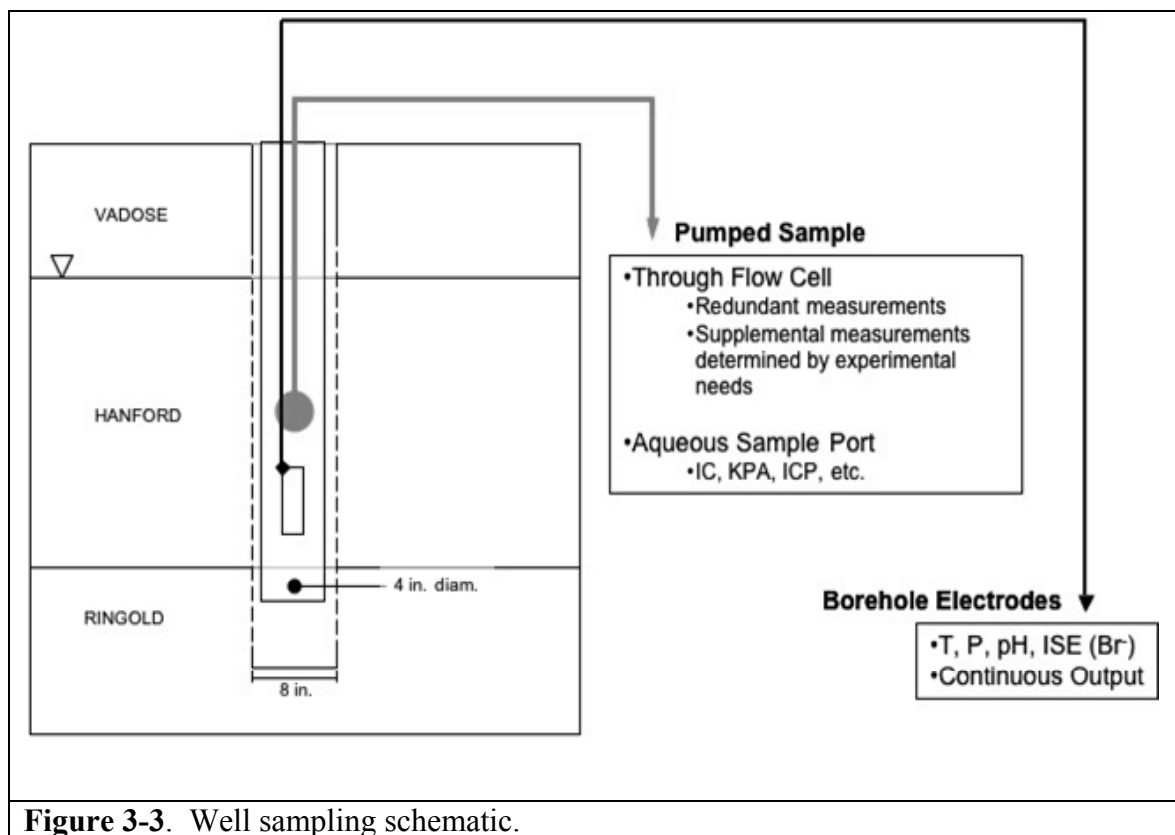


Figure 3-3. Well sampling schematic.

Data from Opportunity Pumped Samples will be used to provide an initial evaluation of the utility of the sampling and monitoring system, a first view of the lateral variation in groundwater composition, and to evaluate the feasibility of using 300 Area samples as source water for chemical and isotopic tracer studies.

Timed Pumped Samples. The IFRC is located near the Columbia River, and the elevation of the 300 Area water table fluctuates with river stage. The site laboratory will be functional prior to low water conditions in the Fall of 2008, and the first sampling of site groundwater will target the condition where groundwater is draining to the Columbia River. During subsequent seasonal and shorter-term fluctuations in river stage, the lateral variation in groundwater composition will be determined by timed sampling. Sample conditions will be similar to the initial conditions for Opportunity Pumped samples, except that the component parameter set will be adjusted according to results from previous tests. The remote and downhole sampling system is equipped with a flow cell that can be adapted to include electrodes for specific ions of interest, and aqueous sampling can be adapted to include hypothesis-specific analytes.

Data from the Timed samples will be used as an ongoing record of compositional responses to groundwater levels and river stage over the life of the project.

Multi-Level Samples. Single-sample groundwater compositional data show significant differences across the 300 Area (**Table 3-1**), and the effects on local groundwater levels of changes in river stage are well documented. The Pumped Samples represent an unconstrained mean of groundwater compositions within the sampled well, which is likely weighted toward transmissive strata exposed in the well bore. A passive multilevel sampler (**Figure 3-4**) will be used to determine the vertical heterogeneity in aqueous compositions. The sampler(s) will be set in the saturated zone and allowed to equilibrate for an indefinite period. When conditions are favorable, e.g., observed to a relatively stable (ca. 6-8 h) at a targeted river stage, the sampler(s) will be removed to the surface and the depth-discrete cell contents transferred to the laboratory for analysis.

Data from multi-level samples will be used collaboratively to determine the three dimensional heterogeneity of site groundwater composition over time and river stage. Sampling and analysis will be used also as part of other experimental protocols to aid in determining the effects of preferential flow within the IFRC.

Smear Zone Samples. The water table at the IFRC fluctuates vertically with shifts in river stage, and this shift is dramatic across the seasonal cycle. The sediment-groundwater system in the region of this fluctuation, which may be termed the 'Smear Zone', may represent a dynamic environment for contaminant interaction with solid surfaces, and for microbial activity across rapidly and frequently changing redox conditions. In addition, the

aquifer may be stratified, with vertical laminations of aqueous components, and the surface of the aquifer could be the most active and reactive portion of the aquifer. In particular, microbial nutrients may be enriched in the Smear Zone and could support a relatively active microbial community. Because the water table shifts, the smear zone may include a small, moving, vertical zone of reactivity that cannot be easily measured by depth-discrete sampling. To test whether this is true, a sampling device will be devised that samples the topmost few cm of the aquifer continuously as needed, regardless of the water table's absolute depth.

3.1 Groundwater Monitoring System

The IFRC wells have been equipped with instrumentation to allow on-demand sampling as needed to follow the trajectory of a rapidly moving groundwater plume (**Figure 3-3**). Components of this sampling and analysis system and its application to groundwater analysis are described below.

3.1.1 Sampling Pumps

Dedicated Grundfos RediFlo2 sampling pumps or comparable will be installed in all site monitoring wells. The sample tubing from each of these sampling pumps will be routed inside an onsite mobile laboratory (or support trailer) and connected directly to a sampling manifold. In the event RediFlo2 pumps are used, sample pumps will be operated using a manufacturer-supplied variable-speed control box (converts standard 110-V single-phase power into three-phase power to meet the requirements of RediFlo2 sampling pumps) and a project-developed multichannel interface (pump switch box) that allows multiple sample pumps to be operated using a single control box. If a different type of sampling pump is used, a comparable multichannel switchbox will be developed to facilitate efficient high frequency sampling of multiple monitoring wells.

3.1.2 Sampling Manifold

A sampling manifold will be used that allows all sampling streams to be routed into a central flow cell for monitoring field parameters and sampling port for the collection of groundwater samples. The advantage of this type of system is that all field parameter measurements are made using a single set of electrodes, which improves data quality and comparability of spatially distributed measurements. Consistent labeling between the sampling manifold and pump switch box simplifies selection of the well to be sampled and reduces the chance of operator error during the frequent sampling associated with the injection experiments.

Table 3-1. Composition of 300 Area groundwaters collected from various excavations in February through April, 2003.

	618-5 Pit 1 (26 Feb 03)	618-5 Pit 1 (29 May 03)	618-5 Pit 2 (26 Feb 03)	SPP Pit 1 (19 Apr 03)	SPP Pit 2 (19 Apr 03)	NPP Pit 1 (26 Apr 03)	NPP Pit 2 (26 Apr 03)	Range
pH	7.71	8.11	7.80	7.83	8.04	7.83	7.88	7.71 - 8.11
Ionic Strength (mmol/L)	7.5	8.2	7.5	3.5	4.9	5.2	6.3	3.5 - 8.2
<u>Cations</u> (mmol/L)								
Ca	1.31	1.17	1.24	0.60	0.90	1.01	1.14	0.60 - 1.31
K	0.16	0.20	0.16	0.07	0.09	0.07	0.06	0.06 - 0.20
Mg	0.58	0.49	0.56	0.21	0.28	0.34	0.40	0.21 - 0.58
Na	1.34	2.65	1.53	0.77	0.95	0.84	1.14	0.77 - 2.65
<u>Anions</u> (mmol/L)								
Cl ⁻	0.84	1.21	0.76	0.14	0.36	0.36	0.39	0.14 - 1.21
NO ₃ ⁻	0.42	0.53	0.40	0.36	0.40	0.29	0.43	0.29 - 0.53
Inorg. C	2.47	2.71	2.41	1.20	1.70	2.02	1.58	1.20 - 2.71
SO ₄ ²⁻	0.69	0.76	0.85	0.35	0.43	0.47	0.88	0.35 - 0.88
Si _{Total}	0.57	0.59	0.55	0.28	0.39	0.32	0.23	0.23 - 0.59
U (μmol/L)	4.96	1.39	1.82	0.30	0.36	0.30	1.07	0.30 - 4.96
Species	(%)	(%)	(%)	(%)	(%)	(%)	(%)	
UO ₂ (CO ₃) ₂ ²⁻	5.8	2.8	5.4	22.0	6.2	7.1	7.3	
UO ₂ (CO ₃) ₃ ⁴⁻	3.5	5.0	4.0	6.5	4.7	4.0	3.9	
Ca ₂ UO ₂ (CO ₃) ₃ ⁰	90.6	92.2	90.5	70.4	88.9	88.7	88.6	
P _{CO2}	-2.559	-2.912	-2.656	-2.971	-3.035	-2.754	-2.913	

3.1.3 Field Parameter Measurements

Field parameters will be monitored using pH, oxidation-reduction potential (ORP), temperature, specific conductance (SpC), and dissolved oxygen (DO) electrodes installed in a flow-through monitoring assembly. The flow-through assembly has been designed to minimize the amount of “dead space” within the monitoring chamber and results in flow-through residence times of less than three seconds under standard monitoring conditions. Purge volumes pumped prior to sample collection will be determined by monitoring stabilization of field parameters. The field parameter monitoring electrodes that will be used during this field test will meet the specifications shown in Section 4.

3.1.4 Groundwater Sample Collection

Groundwater sample collection will be conducted using the equipment described above. The groundwater sampling equipment consists of dedicated variable-speed submersible sampling pumps installed in all site monitoring wells with sample tubing and control wiring routed to a central location inside the onsite mobile laboratory where groundwater field parameters are monitored (in a flow-through cell) and groundwater samples are collected.

The procedure for monitoring field parameters and collecting groundwater samples using this equipment is described below:

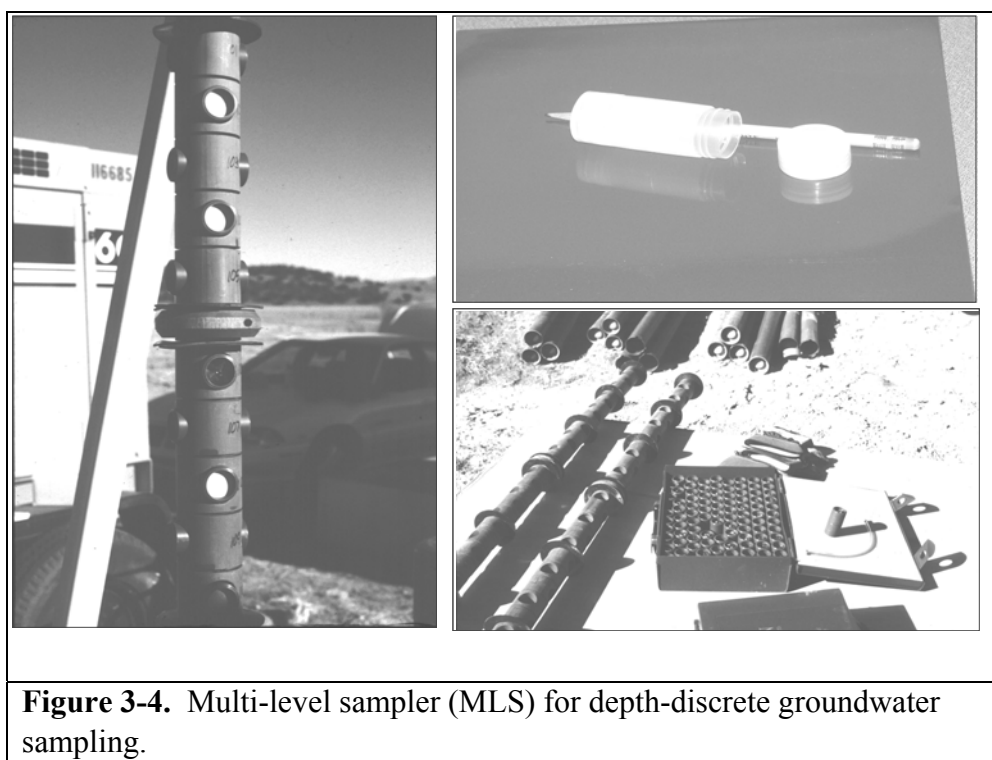
- Select well to be sampled on pump switch box and sampling manifold.
- Start pump at predetermined purge rate (~4 to 8 L [1 to 2 gal] per minute).
- Following displacement of any air bubbles trapped in the sample tubing (generally within the first 20 to 30 seconds), divert ~ 2 to 8 L (0.5 to 2 gal) per minute of sample stream to flow-through cell.
- Monitor field parameters until they have stabilized.
- Record field parameter measurements in field log book or project-specific data sheets and collect required groundwater samples.
- Select next well to be sampled and repeat process.

3.2 Vertical Solute Distributions by MLS

The passive multilevel sampler (MLS) consists of an assembly of non-metallic supports and membrane-capped sample cells (**Figure 3-4**). The support assembly fits snugly within the well screen, and includes centralizers to position the support uniformly within the screen. The samples are collected in cylindrical sample cells capped with filter papers of variable screen size. The sample cells are filled with deionized water prior to placement. After placement in the screen interval, the deionized water equilibrates with the water within the adjacent screen interval, which in turn equilibrates with the surrounding formation pore water. Sample intervals are separated within the screen interval by flexible baffles. The MLS therefore provides a means to sample discrete depth intervals within the aquifer’s aqueous phase.

The procedure for using the MLS is as follows:

- Determine desired sample interval and position baffles on the support rod over the desired sample depth.
- Fill sample cells with deionized water and cap with filter material of desired composition and pore size. A tracer may be included in the fill solution.
- In the field, place the sample cells on the support rod
- Lower the assembly into the well screen to the desired sample-depth interval
- Allow sufficient time for cell equilibration. In transmissive sediments, several days is sufficient.
- Under targeted hydrologic conditions (e.g., low river stage), remove assembly from the well.
- Uncap each cell and transfer the contents to prepared sample vials for analysis



3.3 Smear Zone Water Quality Measurements

Groundwater compositions within the Smear Zone will be collected floating a sample intake device on the aquifer surface, and collecting a time series of aqueous samples whose composition will be contrasted with the pumped and depth-discrete samples from the MLS. The sampler will consist of a down-hole, small-volume pump attached to a bob that can float freely on the aquifer surface. The pump will either run continuously, or will be switched on and off at desired sampling times, to collect samples from the aquifer surface.

3.4 Baseline Water Quality Measurements

The analysis of groundwater samples will include a standard set of compositional parameters (**Table 3-2**). These components will allow calculations of charge balance, aqueous speciation, saturation indices of mineral components, and environmental conditions and contaminant concentrations. The data will be compiled and entered into the IFRC database along with calculated parameters and documentation of the methods or software used to calculate the derived parameters.

Table 3-2. Baseline groundwater chemistry sampling requirements.

Parameter	Media/ Matrix	Sampling Frequency	Volume/ Container	Preservation	Holding Time
Major Cations: Al, As, B, Ba, Bi, Ca, Co, Fe, K, Mg, Mn, Ni, Zn, Zr, P, Sr, Na, Si, S, Sb	Water	Two to three baseline sampling events	20-ml plastic vial	Filtered, HNO ₃ to pH <2	60 Days
RCRA/Trace Metals: Cr, Cu, As, Se, Mo, Ag, Cd, Pb, ²³⁸ U	Water	Two to three baseline sampling events	20-ml plastic vial	Filtered, HNO ₃ to pH <2	60 Days
Anions: Cl ⁻ , Br ⁻ , SO ₄ ²⁻ , PO ₄ ³⁻ , NO ₂ ⁻ , NO ₃ ⁻	Water	Two to three baseline sampling events	20-ml plastic vial	Cool 4°C	45 Days
pH	Water	Monitored during each sampling event	Field Measurement	None	N/A
Specific Conductance	Water	Monitored during each sampling event	Field Measurement	None	N/A
Dissolved Oxygen	Water	Monitored during each sampling event	Field Measurement	None	N/A
Oxidation-Reduction Potential	Water	Monitored during each sampling event	Field Measurement	None	N/A
Temperature	Water	Monitored during each sampling event	Field Measurement	None	N/A

N/A = Not applicable.

3.5 Hypothesis-Based Water Quality Measurements

As information is collected and evaluated, additional measurements of targeted analytes will be made. Early considerations are represented in **Table 3-3**, and include analyses to test whether isotopic tracers inherent to the 300 Area can be used (U isotope measurements) and whether microbial activity acts anaerobically under micro-environmental conditions to produce sulfide or methane. The list in **Table 3-3** will be amended as research requires.

Table 3-3. Experiment-specific groundwater chemistry components.

Parameter	Media/ Matrix	Sampling Frequency	Volume/ Container	Preservation	Holding Time
Fé, Mn Isotopes	Water	As needed	20-ml plastic vial	Filtered, HNO ₃ to pH <2	60 Days
U, O, C Isotopes	Water	- As needed - To evaluate tracer properties	125 ml plastic vial	Filtered, HNO ₃ to pH <2	60 Days
Dissolved Gases (methane, hydrogen)	Water	As needed	Gas sample bulbs	N/A	Same Day
Sulfide	Water	As needed	20-ml plastic vial	Zinc Acetate	60 Days
N/A = Not applicable.					

4.0 Field Hydrologic Properties

The primary objective of the IFRC hydrologic testing program is to characterize the field-scale hydraulic and conservative transport properties for the site, and provide a measure of the spatial variability in these properties. Information obtained from these initial characterization activities will be used to plan for and design subsequent injections of variable temperature waters, field-scale reactive tracer and uranium mass transfer experiments, and later in-situ microbial ecology and response studies.

4.1 Injection System Components and Operation

Constant-rate injection tests and nonreactive tracer experiments will be performed as part of the hydrologic testing and site characterization program. The infrastructure and equipment needed for these large field experiments is described in this subsection.

4.1.1 Water-Level/Pressure Response Measurements

Pressure transducers (5 to 20 psi, 0.1% of full-scale accuracy) will be installed in selected wells to monitor pressure response during hydraulic and tracer injection tests and continuously recorded using a Campbell Scientific CR10 data logger, or comparable. Transducer readings will be validated periodically with water-level measurements to check for transducer drift. Water levels will be measured using a high-accuracy, National Institute of Standards and Technology traceable, non-stretch, metal-taped, water-level meter marked in 0.03.04-cm (0.01-ft) gradations.

4.1.2 Injection Manifold

The injection system consists of an injection pump and appropriately routed piping, valving, and flow rate monitoring equipment. The manifold is used to control (both rate and concentration), monitor, and sample the injection solutions. The manifold will be constructed of 316 stainless steel (or Sch80 PVC) and will use stainless steel ball valves for both diversion/shutoff and flow control valves.

4.1.3 Injection Pump

An appropriately sized feed pump (centrifugal or positive displacement) will be used for injecting the concentrated tracer solution into the make-up water stream. The injection tubing that extends from the well head to the bottom of the test interval will be perforated over the full injection interval and constructed of appropriately sized stainless steel or PVC pipe.

4.1.4 Flow-Meters

Omega turbine flow meters will be used to measure the flow rate of the various streams and the total injection flow rate. Depending on the design injection rate, either a 2.5- or 5.0-cm (1- or 2-in.) diameter flow meter will be used to monitor the dilution water and total injection rate and a 2.5-cm (1-in.) diameter flow meter (or smaller) will be used to monitor the injection rate of the concentrated tracer solutions. These flow meters will be continually logged with a Campbell Scientific CR10 data logger. In the event that a small variable area flow meter (also known as a Rotameter) is used to monitor the injection rate of a small-volume metering pump, these data will be manually recorded on field data sheets.

4.1.5 Submersible Extraction Pump

An appropriately sized stainless steel submersible pump will be used as the extraction pump to supply groundwater from a nearby well for hydraulic testing and tracer solution make-up water. The extraction pump will be installed on an appropriately sized stainless steel riser.

4.1.6 Injection Experiment Procedure

All injection testing will be conducted using the equipment described above. During the non-reactive tracer experiments, the desired injection concentration will be achieved by pumped-injection mixing of the concentrated tracer solutions with dilution water from the extraction well. The extraction well will be selected based on its proximity to the site and the similarity of the uranium isotopic signature of the supply and IFRC site waters. The overall injection pressure for the, mixed concentrated tracer solutions and water from the extraction well will be provided by control of a tracer feed pump and the extraction pump, respectively.

The two injection streams will be mixed within the injection manifold before the solution arrives at the point of injection (i.e., the injection well's screen interval).

All injection flow rates (concentrated solution, dilution water, total) will be monitored with turbine flow meters and controlled by manually adjusting flow control valves. Sample ports will be located on the manifold so that samples of the injection solution can be collected throughout the injection test.

4.2 Hydrologic Testing

Aquifer hydraulic tests will be performed in all IFRC injection/monitoring wells. The hydraulic testing program will consist of a phased approach, the initial phase of which involves the monitoring of hydraulic response during well development activities. Pressure responses observed during developmental pumping, which will provide a qualitative measure of the variability in hydraulic response across the site, will be utilized to guide development of a testing program for the entire well field.

Following well development activities, electromagnetic borehole flowmeter (EBF) surveys (Molz et al. 1994; **Figure 4-1**) will be performed over each aquifer test interval, with measurements taken at ~30 to 60 cm depth increments. EBF data will characterize the vertical distribution of horizontal hydraulic conductivity at each well location and allow the bulk hydraulic conductivity measurements determined from aquifer tests to be partitioned into depth-discrete values that can be used for geostatistical analyses and subsequent groundwater flow and transport modeling (Li et al. 2008, Fienen et al. 2004, Vermeul et al. 2004).

Experience with the LFI and polyphosphate treatability test wells in the 300 Area indicates that slug testing in the very high permeability Hanford formation sediments may not yield definitive or reliable results (Vermeul et al. 2007; Williams et al. 2007). Subsequently, the next phase in the IFRC hydraulic testing program will be focused on conducting constant-rate injection experiments (i.e., comparable to a constant-rate withdrawal, or pumping test) to provide for quantitative hydraulic property estimates. Although conducting a constant-rate injection experiment at each IFRC well location may be cost prohibitive, tests in a subset of wells identified by successive results within the IFRC will be conducted as required to quantify the



Figure 4-1. Electromagnetic borehole flowmeter (EBF) (www.qec-ebf.com).

variability in hydraulic property estimates across the site. The field site is close enough to the Columbia River that analyses of aquifer hydraulic data will need to consider the effects of river stage fluctuations that occur during the experiments. Hydrologic data will be analyzed using peer reviewed analytical or numerical methods that are applicable to the specific conditions encountered at the time of experimentation.

4.3 Non-Reactive Tracer Experiments

Tracer experimentation will be conducted both within the saturated zone as tracer injection and drift tests, and within the vadose zone as tracer infiltration tests. The objective of the IFRC tracer testing/characterization program is to further evaluate formation heterogeneities present in both the vadose and saturated zones, to assess variably saturated transport processes in the vadose zone and transport processes in the saturated zone (including downgradient transport of the tracer plume under natural gradient conditions), to refine the site conceptual model and associated numerical models, and to test operational procedures. These characterization experiments are distinct from those that will be described in the IFRC Field Site Experimental Program, a program plan that is under development.

Tracer testing in the saturated zone will be the first characterization target that will provide information on the effective porosity of the aquifer at the IFRC site and arrival times at the monitoring wells. Results from these experiments will help determine the injection volume and sampling frequency requirements for subsequent field-scale reactive tracer and uranium mass transfer experiments that are planned for the near future in FY 09. An additional benefit of the tracer testing program is to help test equipment operation and procedures needed for subsequent, more complex reactive transport experiments.

For the saturated zone test, a solution containing the conservative tracer, e.g., potassium or sodium bromide (~80 ppm Br⁻), will be prepared and injected into a selected injection well. Due to the extensive array of thermistors that has been installed at the IFRC site, warm or cold water injections are also being considered as a possible tracer. A tracer volume will be used that assures arrival at nearby operational monitoring wells. Bromide concentrations will be measured in the surrounding monitoring wells and breakthrough curves (time vs. concentration) will be measured for each well. The volume of tracer solution required will depend on the saturated zone thickness and planned radial extent of the tracer plume. The injected tracer plume will then be tracked by sampling selected monitoring wells as it moves downgradient under natural flow conditions. Sampling requirements for the planned tracer experiments are shown in **Table 4-1**. Bromide concentrations will be measured using ion selective electrodes (ISE), both in a bench-top flow-through cell for analyzing aqueous samples and in-situ using downhole ISE probes. Archive samples will also be collected as described in **Section 3.0** and submitted to PNNL laboratories for verification of Br-concentration by ion chromatography. For thermal tracer injections, groundwater

temperature measurements will be performed in-situ with dedicated depth-discrete thermistors.

In addition to the saturated zone tracer test, a tracer infiltration test will be conducted in the vadose zone. The test will be conducted through a radially distributed application of a conservative tracer solution at ground surface. The spatial extent of the infiltration gallery and application rate will depend on sediment properties measured in site core samples (see **Section 5.1**) and numerical simulations that incorporate these and other site characterization data (e.g., borehole geophysics, cross-well ERT measurements). Monitoring of the wetting front will be accomplished through spatially distributed depth discrete cross-well ERT measurements and localized measurements with a neutron probe. Based on the timing of this test, either a Br⁻ tracer or alternate salt tracer (e.g., Cl⁻) will be used. The advantage of using a Br⁻ tracer would be that the saturated zone monitoring equipment would already be configured to assess tracer released from the infiltration test and subsequent downgradient movement of the tracer plume through the saturated zone. However, if test timing is such that there is expected overlap between tracer plumes resulting from the two tests, an alternate tracer would be utilized and saturated zone monitoring reconfigured accordingly.

Table 4-1. Tracer injection test sampling requirements.

Parameter	Media/ Matrix	Sampling Frequency	Volume/ Container	Preservation	Holding Time
Anions: Br ⁻	Water	Determined based on predicted tracer arrivals	20-ml plastic vial	Cool 4°C	45 Days
Br ⁻ Field Screening	Water	Determined based on predicted tracer arrivals	Field Measurement	None	N/A
pH	Water	Monitored during each sampling event	Field Measurement	None	N/A
Specific Conductance	Water	Monitored during each sampling event	Field Measurement	None	N/A
Dissolved oxygen	Water	Monitored during each sampling event	Field Measurement	None	N/A
Oxidation-Reduction Potential	Water	Monitored during each sampling event	Field Measurement	None	N/A
Temperature	Water	Monitored during each sampling event	Field Measurement	None	N/A
N/A = Not applicable.					

5.0 Laboratory Characterization of Core Materials

5.1 Core Samples and Characterization Strategy

Well construction at the IFRC experimental site has collected intact cores and grab samples. **Table 5-1** (from Bjornstad and Horner 2008) summarizes the numbers and types of samples that were targeted for collection by the drilling operation. The intact cores have been sealed in 1-foot lexan liners and stored under cold room conditions for future experimentation and distribution to investigators. More than 100 total individual core segments have been collected from seven ‘characterization’ wells. Bulk-sediment grab samples have been collected at 2-foot intervals by distributing continuous well cuttings into 5 gallon plastic buckets (‘Bucket Samples’). More than 700 of these samples have collected, dried to field-moist conditions, and stored at ambient temperature. This inventory of core and grab samples referenced to specific well number as shown on **Figure 1-2** is posted on the Hanford IFRC website under “*IFRC Geologic Sample Final Inventory*”.

A catalogue of processed samples is being constructed for access on the IFRC website. The catalogue will include information on sample collection, position, geologic description, processing history, and available sample mass. Registered investigators will be provided with an online mechanism to request specific samples, and sample distributions will be accessible to all investigators. Details of the sample request process will be posted on the website as the system becomes available.

Table 5-1. Drilling, sampling, and well-completion information for 35 new IFRC wells.

New IFC Wells										
Type	# Wells	Preferred Drill Method	Total Depth (ft)	Borehole Diameter	Screen	Screen Interval (ft)	Proposed Sampling	Total # samples/well	Total # samples	Comments
ERT-instrumented/gw monitoring <i>without</i> core collection	18	cable tool or sonic	58	8"	4" PVC	31-56	Grab samples every 2 ft	29 grab samples*	464 grab samples*	sandpack below 10' depth; one well to be used as saturated-zone injection well
ERT-instrumented/gw monitoring <i>with</i> core collection	7	sonic	58	8"	4" PVC	31-56	4 holes continuous core in 0.5 ft lexan liners within 5-ft long, min. 4-in ID split spoon; liners; 3 holes collected in 2-ft long sections of lexan, approximately the same diameter as the core barrel OD, at surface (i.e. grab samples)	12 split spoons or 58, 1-ft lexan liners; 29, 2-ft core samples	84 split spoons or 406, 1-ft lexan liners; 203, 2-ft core samples	continuous core (min 4' OD); sandpack below 10' depth
3-well cluster (multi-level) gw monitoring	3 clusters	cable tool or sonic	37, 46, 57	8"	4" PVC	30-35, 42-44, 53-55	Grab samples every 2 ft	66 grab samples/cluster*	198 grab samples*	ERT on deep (56 ft) well only (sandpack below 10' depth)
Deep characterization; gw monitoring	1	sonic	~180	8"	4" PVC	60-140	~60 ft of core collected in lexan liners, from five intervals (30-35', 50-70', 95-100', 122'-132 ft, and 170 ft to TOB); grab samples every 2 ft between core runs		Up to 12, 5-ft split-spoon segments; 60 grab samples	Continuous screen to test groundwater across redox boundaries in Ringold Formation
Total wells	35						*collected at surface by emptying core barrel into 5 gal. buckets or capped lexan liners (if collected by the sonic method use 2-ft long sections of lexan, approximately the same diameter as the core barrel OD)			

The objective of baseline characterization is to provide an estimation of the site's three-dimensional variability in lithology, geochemical, and hydrologic properties. The resultant information will be used to formulate more detailed hypotheses on field factors controlling reactive transport. For measurements and distribution where time and sample preservation are critical, a limited number of core samples (based upon requests and their justification, collectively reviewed by IFRC Investigators) will be breached and sampled proximate to the end caps. However, baseline characterization will rely primarily upon Bucket Samples. To produce a preliminary characterization data set within a reasonable and early period, the initial characterization effort will focus on 200 samples selected from the total inventory of Bucket Samples. Collection of continuous well cuttings will produce approximately 20 Bucket Samples from below backfill (approximately 4 m bgs) to 1 m below the Hanford-Ringold contact for each of the 35 wells. The full set of samples from 3 wells (approximately 60 from 2-18, 2-29, and 3-30, **Figure 1-2**) will initially be characterized to provide data from comparable depths over the entire stratigraphic column. Another 40 samples will be taken from nearby cluster wells 2-26, 2-31, and 3-32 that are being composited for USGS study.

The remaining 100 samples will be Bucket Samples of saturated zone sediments from different wells that span the range of extant lithologies/facies at the IFRC site as determined by spectral gamma logging spectroscopy (SGLS). These 100 samples will be selected in consultation with those developing the geostatistical model to assure that the integrated sample set will yield the most rigorous spatial representation of the site. This initial characterization data set of 200 samples may be further augmented to enhance the robustness of the IFRC geostatistical model.

Bucket samples will require processing prior to storage, to remove water from saturated-zone samples, and to estimate the grain size distribution at the IFRC. All Bucket samples will be processed as described below, and the information collected during processing will be an integral part of the characterization data set.

5.2 Geologic Analysis

The conceptual hydrogeologic model of the IFRC site shall be constructed based the extensive geologic and hydrologic information gathered during drilling, field sampling, and geophysical logging of the 35 IFRC wells. Previously drilled wells in the vicinity of the IFRC site shall also be integrated into the model where appropriate. Data to feed into the model will include:

- Geologist's logs, which describe sediment classification, estimate of grain size distribution, color, moisture, mineralogy, and diagenetic alteration, as well as lithologic-contact information for each stratigraphic unit or boundary
- Well-construction information and location of down-hole ERT and thermistor sensors

- Geophysical logs (spectral gamma, total gamma, neutron moisture), often a reflection of lithologic and moisture conditions
- Core and grab-sample photographs
- Sample Inventory

These data for the new IFRC wells are presently being compiled into a Borehole Drilling, Sampling and Well-Construction Report.

The geologic data will be summarized onto a single log sheet for each of the 35 wells. Integrating all the information for each individual well onto a separate log sheet, at the same scale, allows for a quick, easy evaluation of differences and similarities of the wells and sampling points. A number of scaled hydrogeologic cross sections will be constructed at various locations through the site, showing how various lithofacies might correlate across the site. This will provide a basis from which to evaluate stratigraphic lithofacies correlations between wells based on down-hole electrical resistivity and other remote-sensing techniques. Using lithologic contact information from the summary logs, plan-view isopach and structure-contour maps will be generated showing the variations in thickness and attitude of the various stratigraphic units and contacts, particularly the attitude of the high-contrast contact between the Hanford and Ringold formations. Contact data will also be input into an Earthvision® (3-D visualization software) model, which allows for rapid, easily generated cross-sectional and cutaway views of the subsurface from any aspect or inclination angle.

5.3 Processing and Screening of IFRC Well Samples

5.3.1 Continuously Cored Wells

Continuous samples were collected by split spoon coring. Each core interval within the drill string was sampled into five collinear one-foot long, four-inch diameter lexan liners. The liners were individually separated at ground surface from the inclosing five-foot metal split spoon and capped with tape seal (see photographs on web site). The intact liners were weighed onsite and moved to the walk-in cold storage facility at the PNNL RTL Building. These materials are stored at 4 °C for future research. Any IFRC investigator may request specific intact core samples listed in the inventory for their research. The project requests that at least one 100 g subsample be archived from each core for basic characterization measurements.

For distribution of core samples to IFRC Investigators, a collaborative arrangement will be made to minimize sample numbers and maximize measurement types. For example, removal of a subsample from a core interval for microbial experimentation might be coupled with sampling for moisture content and geochemical properties.

5.3.2 Bucket-Sampled Wells

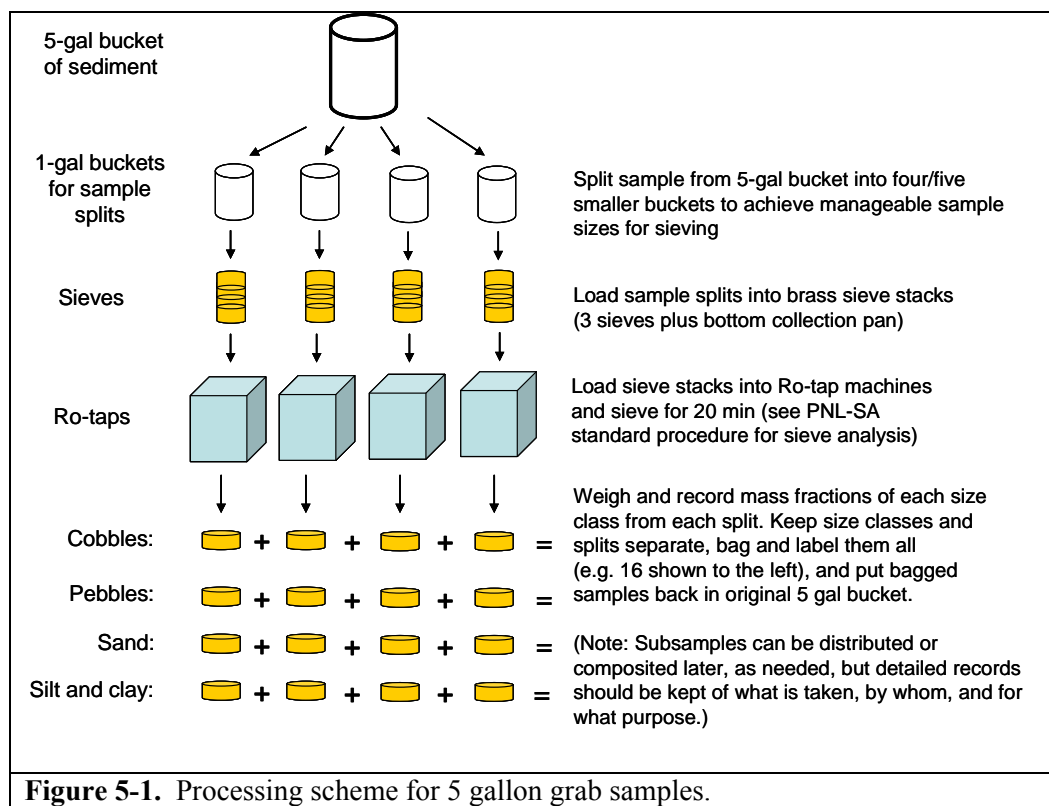
Samples were collected from the core barrel advanced without liners. The cored material was vibrated from the core barrel into a plastic sleeve, in 2-foot intervals. The material was displayed on a table for geologic description. Grab samples were collected into five gallon plastic buckets and weighed onsite. The Bucket Samples were moved to a suitable location for further processing. Bucket weights range from 6-12 kg.

Storage of Bucket Samples:

1. Vadose Zone: Stored field moist at ambient temperature.
2. Saturated zone: Spilled onto a plastic covered table and allowed to dry to field moist conditions, then stored at ambient temperature.

Processing Bucket Samples (See **Figure 5-1**):

1. Spread onto plastic covered table and physically quartered to preserve overall size distribution (saturated zone samples allowed to dry to field moistness before further processing.)
2. One quarter preserved as a reserved archive.
3. Remainder dry sieved into four size fractions: Silt-Clay (<62 μm = 4 phi, passes no. 230 sieve); Sand (62 μm – 2mm = -1 phi, passes no. 10 sieve); Pebbles (2mm – 64mm = -6 phi, passes 63mm sieve); Cobbles (>64mm = won't pass 63mm sieve).
4. As size-fraction quantity permits, divide each fraction into halves, one for immediate availability to Investigators, and one for distribution after completion of initial characterization.
5. Report all subsample weights and sample numbers.



5.4 Physical Property Measurements

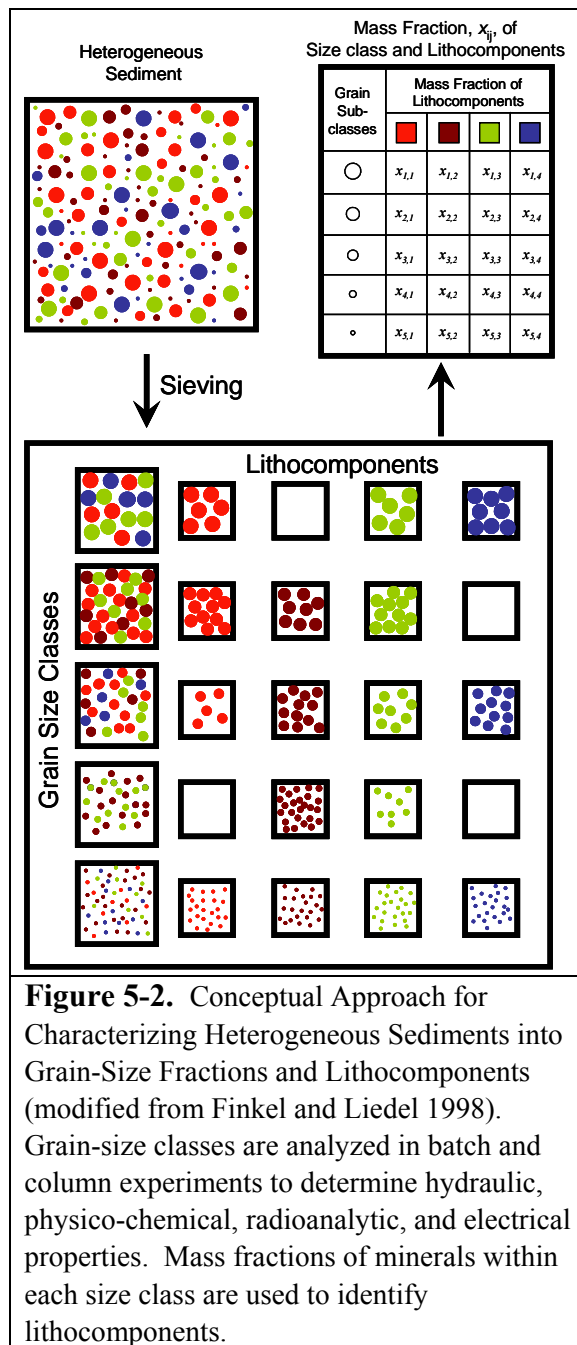
The characterization effort for the IFRC site is based on the premise that physicochemical, geophysical, and hydraulic properties at the site are functions of fundamental properties including the grain-size distributions of the sediments and related attributes such as mineralogy. Measurements will therefore be performed to quantify relationships between grain size metrics and related attributes to define various property transfer models. In soil science disciplines, these types of property transfer models are sometimes called *pedotransfer functions*. In the petroleum exploration and production industry property transfer models may be referred to as *petrophysical relationships*.

Unlocking the power of property transfer models for predicting key model input parameters from easily measured properties (e.g., grain size distribution and geophysical responses) requires a higher level of sediment characterization than is typically performed. Understanding the contribution of each textural subclass to the lithology, hydraulic, physicochemical, and radiometric properties is a prerequisite to understanding their contribution to effective properties of the heterogeneous sediments. Laboratory measurements will be performed on 200 samples to characterize various hydrogeophysical properties and to establish a database of fundamental properties (e.g., particle shape, mineralogy, porosity etc). Property transfer models will be developed from these fundamental properties and from laboratory and field-scale observations.

5.4.1 Sample Processing

This approach to sediment characterization, illustrated schematically in **Figure 5.2**, involves the separation of heterogeneous sediments into characteristic grain-size fractions, with subsequent determination of the lithologic composition (i.e., mass fraction of component minerals) and properties of each size fraction. Heterogeneous samples will be separated by sieving and sedimentation techniques into the four main textural classes, gravel, sand, silt, and clay, and subdivisions of these classes. Owing to the high gravel content of 300 Area IRFC sediments, gravel can be expected to play a major role in determining the effective flow and transport properties. Therefore the coarser textural classes will be divided into five subclasses (very coarse, coarse, medium, fine, and very fine) as represented in **Figure 5-2**. Each subclass will then analyzed to determine the mass fraction of lithocomponents and to characterize hydraulic, physico-chemical, radiometric (e.g., gross, natural radioactive elements ^{40}K , ^{238}U , and ^{232}Th , and their ratios) and impedance (complex resistivity) properties.

Following decomposition of the sediment into the component phases and characterization of representative facies, sediment size separates will be used to generate model mixtures for batch/column measurements. This approach is based on the principle that the borehole log and surface geophysical responses are related to the sum of proportions of the lithocomponents, each multiplied by the appropriate response coefficients in a system of linear equations that can be solved simultaneously. Laboratory measurements will characterize a variety of physico-chemical, geophysical, and hydraulic parameters of the whole and sieved soil samples using methods described below.



5.4.2 Particle Size Distribution

Two methods will be used to determine particle size distribution (PSD): 1) mechanical analysis by sieving, and 2) laser diffraction spectrometry (LDS). Sieve analyses will be performed initially on 200 bucket samples of the bulk sediments.

Sediment samples will be separated into four primary grain-size fractions, namely, gravel, sand, silt, and clay and sub classes based on the logarithmic Udden-Wentworth grade scale (Wentworth 1922). Dry sieving will be used to separate the sediments above 2000 μm into the very coarse, coarse, medium, fine, and very fine subclasses of the gravel. Approximately 500 grams of each sample of interest will be placed on a sheet of brown shipping paper laid out on wires racks to air dry over a 48-hr period. The gravel sieve stack will include the 2 -1/2", 1-1/4", 5/8", 5/16", # 5 sieves and a pan. Each sample will then be sieved through the gravel sieve stack for about 30 minutes at 3,000 oscillations/min, and the mass of sediment retained on each sieve recorded. The sediment collected in the pan will then be used for wet sieving on a sand sieve stack (#10, #18, #35, #60, #120, #230) and LDS analysis. The LDS measurements will be performed with a Mastersizer 2000 (Malvern Instruments, Inc., Southborough, MA) using the wet dispersion method. The ultrasonic processor will be used for particle-size reduction and disintegration of aggregates (sonication). These data will be combined with the dry sieve data to generate a complete particle size distribution curve. The percentage of each size fraction will then be used to determine grain-size moments and to assign facies.

5.4.3 Particle Shape

Particle shape is important to the packing arrangement of particles and therefore to physical properties such as bulk density and porosity. Particle shapes will be determined using angle-of-repose measurements. Granular materials exhibit at least two characteristic angles at rest, a lower angle defined as the angle of repose (ϕ_r) and a maximum angle, ϕ_m , also referred to the angle of initial yield. A variety of studies have shown a strong relationship between slope angles and particle shape as well as between ϕ_r and porosity. In general, ϕ_r reaches a maximum for the minimum porosity. Angle-of-repose measurements will be made in a water-filled Hele–Shaw cell (**Figure 5-3**) constructed such that the accumulation of material inside the cell can be observed and the slope angles measured, based on the design described by Friedman and Robinson (2002).

Repose angle measurements of sediment size fractions will be made by filling the feeder tray with the material of interest and then allowing the material to fall into the water. Pouring under water allows for the creation of well-defined slopes. The entire process will be videotaped to allow observation of the unstable lobe and maximum slope angle. Angle-

of-repose measurements will be made for all the size classes. Independent measurements of porosity will be made to allow correlation with angle of repose.

5.4.4 Porosity

The porosity of sedimentary materials reflects the depositional environment and is a critical parameter for estimating water retention and hydraulic conductivity of heterogeneous subsurface formations. However, the estimation of porosity for Hanford sediments has been difficult. Porosity measurements will be conducted on ~40 intact cores using measured bulk and particle densities, and on ~50 grab samples using the following four-step procedure. First, a 50-g sample of each sediment will be weighed and transferred to a measuring cylinder, and the volume recorded. Next, the contents of the cylinder will be transferred to a second cylinder containing 50 mL of water. The sediment will be left to settle in the water,

after which the combined volume of the sediment and water will be measured. The packing (or bulk) density is calculated as the ratio of the mass to the volume, and the total porosity is calculated as the ratio of the volume of air to the sediment volume. Porosities and densities will be determined for poured (loose) and dense (vibrated) packs of each sediment fraction. These data, along with particle shape and particle density of each fraction, will be used to calculate porosity from particle size distributions of

the grab samples using a packing model. The resulting data can then be used to estimate porosity as a function of depth based on PSDs and borehole logs. Porosity measurements will be determined on core samples by measuring the water content at saturation using time domain reflectometry (TDR) techniques.

5.4.5 Particle Density

Particle density, ρ_s , is widely used for establishing the density-volume relationship of subsurface sediments. Although commonly assumed to be 2.65 Mg/m^3 , the density of quartz, many silicate and non-silicate minerals such as feldspars, micas, smectite, and calcite typical of Hanford sediments exhibit densities between 2.3 and 3.0. The mean particle density of a sediment therefore depends on the mineral composition of the various fractions (**Figure 5-2**) and is calculated using a weighted mean. Particle density, ρ_s , measurements will be performed on three replicates of each size fraction less than 2 mm using the pycnometer

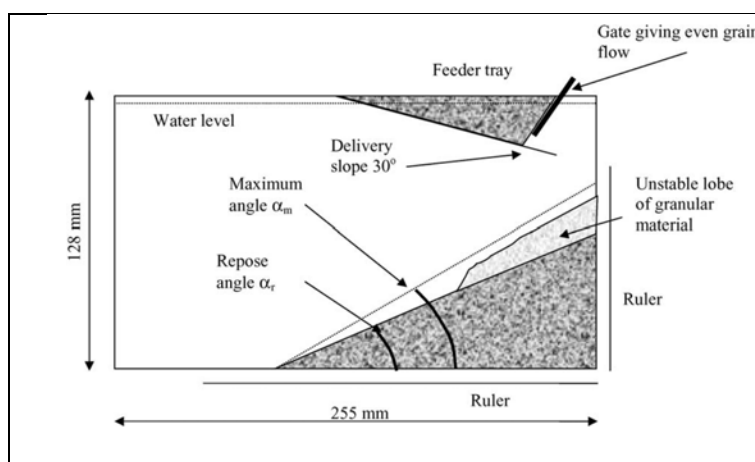


Figure 5-3. Schematic of the Hele–Shaw Cell used to Measure Slope Angles. The angle of repose (ϕ_r) and the maximum angle of stability (ϕ_m) are shown (modified from Friedman and Robinson 2002).

method. The mean particle density of each sample will then be calculated as a weighted sum of the densities from the n size classes.

5.4.6 Specific Surface Area

The specific surface area, SSA, is a measure of the exposed surface of a solid sample and is important for the calculation of surface site concentrations for adsorption reactions, surface conductance of the different lithofacies, and description of water retention at low saturations. Specific surface area will be measured on 25 grab samples using a Quantachrome Autosorb 6-B gas sorption surface area analyzer. The Monosorb is a direct-reading dynamic-flow surface-area analyzer that uses a single-point Brunauer-Emmett-Teller (BET) method to determine the surface area (Brunauer et al. 1938). Standard surface area reference materials will be used to calibrate the instrument over the anticipated range of surface areas. The surface analyzer measures the quantity of a gas adsorbed on a solid surface when it is cooled, with liquid nitrogen, by sensing the change in thermal conductivity of a flowing mixture of an adsorbate (nitrogen) and an inert (helium) carrier gas. With nitrogen and helium, the surface area can be determined down to 0.1 m^2 . With mixtures of krypton and helium, the limit of detection is extended down to 0.01 m^2 . The isotherm points will be transformed with the BET equation and the relationship between equilibrium pressure and the quantity of gas adsorbed used to calculate the surface area.

5.4.7 Saturation-Dependent Properties

Hydraulic, electrical, and thermal properties of soils are sensitive to soil texture and the degree of saturation, among other factors. Characterization of hydraulic, thermal and electrical properties will therefore be combined to allow measurement as a function of water saturation.

Water-retention measurements will be made on 50 intact samples using a modified controlled volume technique (Winfield and Nimmo, 2005). This method is ideal for large, undisturbed samples. The controlled volume method allows determination of points on the water retention curve by extracting or adding water to a sample in fixed-volume increments and allowing the pressure head to equilibrate (**Figure 5-4**). During each time step, a known volume of water is extracted (for drying curve) or added (for wetting curve) to bring the sample to a known average water content.

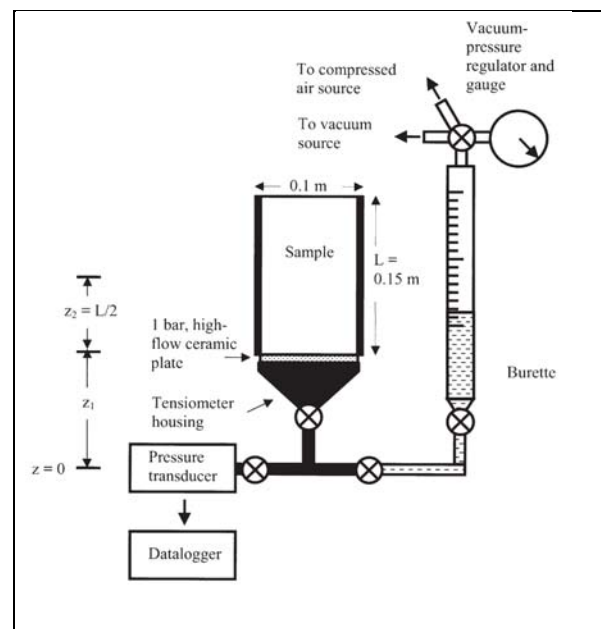


Figure 5-4. Schematic of apparatus used for rapid measurements of water retention using the controlled-volume technique (after Winfield and Nimmo, 2005).

This approach, based on pressure equilibration, is relatively fast because approximately half of the sample de-saturates during a given step. The method is limited to pressures in the range of 0 to -1000 cm-water. The BET adsorption isotherms collected during the specific surface area measurements can be used to extend the water retention function from the measured capillary region to the dry region according to Silva and Grifoll (2007).

The typical controlled-volume apparatus consists of a large tensiometer, a burette, a vacuum-pressure regulator, a pressure transducer, and a data acquisition system. Measurements will be conducted on the intact core liners after saturated hydraulic conductivity measurements are completed (described below). The lower collar is used to attach the column to the tensiometer base. Starting from saturation, points on the drying curve will be obtained by a sequence of steps. First the desired volume of water is removed from the sample by applying suction at the base of the sample. The water content within the sample is monitored using a time domain reflectometry (TDR) probe installed through the side wall. Recording a number of volume and equilibrium-pressure pairs for a particular sample defines points along the drying curve. At the end of the measurements, the sample is oven dried and the weight determined. The dry weight is then used to calculate the sample bulk volume and bulk density.

A measurement apparatus similar to that shown in **Figure 5-4** has been developed and modified to allow for impedance spectroscopy measurements as a function of saturation by replacing the porous ceramic plate with a porous steel electrode. Each electrode is 3.99 ± 0.01 " in diameter and 0.039" thick and is constructed from 316 stainless steel (Mott Corporation, Farmington CT, part number 4300-3.99DIA-.039-0.2-A) to create a porous plate with a mean pore size of 0.2 μm . A 2" long 1/8" stainless steel wire is welded to each electrode, about 1 inch from the outer edge to allow connection to the instruments. For two electrode resistivity measurements, the stainless steel electrodes at the top and bottom of the sample are used. For 4-electrode measurements, an additional two electrodes will be installed through the sidewall such that the spacing between the 4 electrodes is 3 cm. The two additional electrodes will be constructed for the dual purpose of measuring sediment water suction (i.e. a tensiometer) as well as acting as non-polarizable electrodes for 4-electrode electrical measurements.

Electrical resistivity and induced polarization measurements will be made using a Mini-Sting automatic earth resistivity and induced polarization system (AGI Geophysics). The Mini-Sting is a low-cost resistivity and IP meter specially designed for laboratory-scale resistivity surveys and is similar in operation to the Super Sting 8 instrument that will be used in the field surveys. Resistivity and induced polarization measurements will be collected both on intact cores (within 4 in diameter by 6 in long Lexan liners) and grab samples using a 4-electrode configuration based on a Wenner array. Measurements made at the scale used by the Mini-sting system represent a close approximation to the true bulk resistivity and chargeability of the sediment. While resistivity gives information on bulk soil resistivity, the induced polarization (IP) measurement provides the capacitance or chargeability of the

sediment by measuring the variation of voltage with time. The IP data will be used to determine the ground capacitance or chargeability, which is related to soil texture (via surface conductance and cation exchange capacity), and the surface area to pore volume ratio - variables that are related to required input parameters for reactive transport models.

More detailed measures of the saturation-dependent and electrical properties will be made using impedance spectroscopy. This technique is commonly used to characterize micro-structural properties, including the distribution, geometry, and connectivity of conducting phases, (Roberts and Lin, 1997) and grain boundary properties (e.g. MacDonald, 1985; Lockner and Byerlee, 1985). Impedance spectroscopy has also been used to monitor chemical reactions such as ion exchange in soils (e.g. Olhoef, 1979, 1985) and redox changes. Impedance spectroscopy measurements will be made using a Solartron electrical impedance meter and a HP 4284A LCR meter. Both instruments are high-input impedance meters that measure impedance magnitude $|Z|$, phase angle ϕ , resistance R, and capacitance C. The error of measurement for each instrument varies according to frequency and resistance, but is generally less than 1% up to 100 k Ω , and within 5% at the highest impedance limits (> 100 M Ω). The frequency range of the Solartron is 10 μ Hz to 30 MHz whereas the frequency range of the HP 4284A is 20 Hz to 1 MHz.

Two types of impedance measurements will be performed on select samples: 1) measurements on core samples at field moisture to characterize conditions at sampling, and 2) measurements on core samples as a function of saturation. Resistance and capacitance measurements will be made at field moisture content on all cores, after which select cores will be saturated with synthetic groundwater to allow measurements during de-saturation. The synthetic groundwater will be prepared to mimic native waters from the 300 Area. Continuous measurements of resistance and capacitance will be made during desaturation. These measurements will be used to characterize the frequency dependence of the resistivity and dielectric permittivity. These data will be used to identify regions of saturation in which specific conduction mechanisms may be operational. More importantly, these data will be used to identify the saturation at which water transitions from the adsorbed to the bulk state, a transition that impacts flow and transport properties and is related to rate-limited mass transfer.

5.4.8 Measurement of Thermal Properties

Subsurface heat transfer, water movement, and solute transport in the vadose zone are tightly coupled, and characterization of IFRC must therefore consider thermal properties. Moreover, thermal properties measurements are needed for modeling variable temperature groundwater injection and transport at the IFRC field site. Measurement of thermal properties and their saturation dependence will be made using a thermo-TDR probe (Ren et al. 2003; Oschner et al 2001).

The thermo-TDR probe consists of three parallel stainless steel cylinders (1.3-mm diam. and 40-mm length) with a 6-mm distance from the central cylinder to the outer cylinders (Ren et al. 2003). The outer two cylinders enclose thermocouples at the midpoint, and the center cylinder encloses a heater wire. The heater wire and thermocouples are kept in place with high-thermal-conductivity epoxy, which also serves to provide a water-resistant and electrically insulated probe. A coaxial cable is connected to the probe by soldering the positive lead to the central cylinder and the shield to the two outer cylinders. With this design, accurate water content measurements are made using traditional TDR methods. For thermal measurements, a constant current is applied from a direct current supply to the central heater for 15 s to generate the heat pulse. A data logger is used to record the voltage drop across a precision resistor and the temperature in the outer cylinders is measured as a function of time for 300 s. Soil thermal properties are then calculated by analyzing the temperature increase as a function of time using a nonlinear curve-fitting technique. For each sample, the heat-pulse measurements will be repeated three times at 60-min intervals, and thermal properties will be calculated as the average of the three replicate measurements.

5.4.9 γ -ray Spectrometry Measurements

Gamma(γ)-ray spectrometry measurements (of ^{40}K , ^{238}U , and ^{232}Th and their ratios) will be made on whole sediment samples and on their particle size fractions to develop interpretive relationships for the downhole SGLS measurements. About 20 g of each size fraction will be packed into a plastic, radon impermeable Marinelli beaker, sealed and allowed to equilibrate for one week. Breaking or grinding of monolithic samples may cause the release of ^{222}Rn , thereby perturbing equilibrium within the ^{238}U decay chain. To avoid this complexity, gravel samples will be packed into larger Marinelli beakers to avoid having to break individual particles. All samples will be analyzed using 60% efficient intrinsic germanium gamma detectors calibrated for distinct geometries using mixed gamma NIST (National Institute of Standards and Technology) standards. The samples will be counted for 240 minutes in a fixed geometry. All spectra will be background subtracted. Spectral analysis will be performed using libraries of reference spectra containing mixed fission products, activation products, and natural decay products. Control samples will be run throughout the analysis to ensure correct operation of the detectors. Details are listed in PNNL procedure Gamma Energy Analysis, Operation, and Instrument Verification using Genie2000™ Support Software.

5.5 Geochemical Measurements

5.5.1 Initial Geochemical Characterization

A working hypothesis for baseline characterization is that the mineralogic and geochemical variation within the Hanford formation gravels (which comprise the site) is controlled by the energy regime during deposition, through the resultant grain size distribution. (Grain size distribution in the crude approximation embodied within the sieving

procedure outlined above may also provide an estimator of hydraulic conductivity over the site.) Geochemical measurements on Bucket Samples will proceed according to this hypothesis by focusing on the silt-clay and sand fractions of the sieved sediments. Approximately 200 Bucket Samples will be assayed for total U using a fusion and dissolution procedure, labile contaminant U using bicarbonate extraction, U(VI) sorptivity by single-point K_d measurement in two synthetic groundwaters, and poorly crystalline Fe (ferrihydrite) by 0.5 h AHH extraction. Detailed procedures for each sample characterization activity will be posted on the IFRC website; brief method descriptions follow. These extractions will be performed on the combined sand-to-silt fraction of the sieved sediment (e.g., < 2mm).

The characterization effort will be staged according to periodic evaluations of the relative importance of measured parameters. For example, we will proceed on the initial hypothesis that the sand fraction is of less reactive importance than the silt-clay fraction. This hypothesis will be tested by parallel measurements on a limited number of same-sample sand and silt-clay fractions. If the truth of the hypothesis is supported by analytical results, then the analysis of the sand fractions will be discontinued; if the hypothesis is false, all sample analyses will include measurements of the sand and silt-clay fractions.

The total concentrations of U in the <2 mm sediment samples will be determined by fusion and dissolution (Crock and Lichte, 1982), with subsequent ICP-MS analyses (Lichte et al., 1987). For this procedure, the samples are ground (2g), mixed with an equal mass of lithium tetraborate ($\text{Li}_2\text{B}_4\text{O}_7$), and fused in a carbon crucible at 1000°C for 30 minutes. The fusion bead is ground; 250 mg is dissolved in 6 mL HF, 2 mL HNO_3 , and 2 mL of HClO_4 ; and the acid mixture evaporated to dryness at 110°C . The residue is subject to a second evaporation step with 2 mL HClO_4 at 165°C , with subsequent addition of 3 mL HNO_3 , 8 drops of H_2O_2 , 3 drops of HF and an internal standard of In, Re, and Ru (Doherty, 1989) when cooled. The sample is then diluted to 60 mL final volume. The procedure completely dissolves refractory phases such as zircons, garnets, and U-containing Ti-oxides (an important detrital U-containing phase in Hanford sediment; Zachara et al., 2007). Final analysis is performed using a Hewlett Packard model 4500 ICP-MS with plasma power of 1300 watts. Analytical precision based on repeated analyses of international standards (N=54) and given as a coefficient of variation in % (e.g., $\text{stdev/avg.} \times 100$) was 6.51 for U and 1.57 for Zr. Additional details on methodology, precision, and accuracy are available (<http://www.sees.wsu.edu/Geolab/note.html>). Total contaminant U is calculated as the difference between total U and background U (1.6 $\mu\text{g/g}$).

Carbonate extraction will be used to measure labile adsorbed U(VI) as described by Kohler et al., (2004). A mass of 40 g of a carbonate extraction solution with a pH of 9.45, an alkalinity of 20 meq/L and an ionic strength of 0.022 M will be used to extract 2 g samples of dry sediment for 336 h (2 weeks). The 2 week equilibration time is operationally defined, and has been selected based on other repeated analyses of comparable 300 A sediments (e.g., Bond et al., 2007). Samples will be mixed on a shaker table, and a 1.5 mL solution aliquot

removed, filtered, and acidified to 1% HNO₃ with concentrated HNO₃. The U(VI) content in the extracts will be analyzed by a kinetic phosphorescence analyzer (KPA). Approximately 20 samples from the characterization series of 200 will be subjected to time variable extractions out to 2200 h.

Two single point U(VI)-K_d measurements will be performed using two compositions of synthetic groundwater to estimate U(VI) adsorptivity. Numerous U(VI) adsorption isotherms have been measured on 300 A vadose and saturated zone sediments that have shown linear or Langmuir behavior over the relevant concentration range. This background information allows estimation of isotherm behavior from a single-point K_d. The sediment will be washed with synthetic groundwater before K_d measurement until U(VI)_{aq} < 10 µg/L (see Um et al., 2008). The K_d measurement will be performed at 60 µg/L total U(VI) concentration (the average U(VI) concentration found in IFRC groundwater at low river stage) with a 1:2 solid-liquid ratio for 24 h. U(VI), pH, Ca²⁺, and HCO₃⁻ will be measured on the final solution. The electrolytes will be formulated to simulate average low-river and high-river groundwater compositions in the IFRC well domain (based on groundwater sampling and analysis in **Section 3.2**). Example groundwater compositions determined by sampling in 2003 for SPP are shown in **Table 5-2**.

Extractable Fe(III) oxide will be measured by 0.5 h extraction with a hydroxylamine hydrochloride solution (Chao and Zhou, 1983; Coston et al., 1995), a technique that has been used to determine the poorly crystalline Fe oxide content (e.g., ferrihydrite) of aquifer sediments. Duplicate 1 g samples will be extracted with 20 g of 0.25 M NH₂OH·HCl in 0.25 M HCl at 50 °C. Solution aliquots (1.5 mL) will be taken at 0.5 h and immediately filtered and diluted with 1% HNO₃ for ICP-ES analysis. Note that total Fe, Al, and Mn measured in the contaminant U extractions described above will provide semi-quantitative estimate of total crystalline and poorly crystalline Fe, Al, and Mn oxides (contributions from the dissolution of phyllosilicates and other more soluble aluminosilicates are unavoidable given the acidic pH and elevated temperature). Quantitative estimation of these sorbent pools may require specific extraction using different methods that would be performed during secondary characterization of a smaller sample set (described below in **Section 5.5.2**).

Sediment pH will be determined for sand and silt-clay fractions using a 1:1 sediment:solution suspension open to the atmosphere using a pH electrode and meter.

The initial characterization will thus define total and labile contaminant U, U(VI) adsorptivity, reactive Fe(III) oxide content (ferrihydrite), and sediment pH on the < 2 mm size fraction of 200 grab samples.

5.5.2 Secondary Geochemical Characterization

After completion of the initial characterization described above, the results will be examined to determine whether the sand and silt-clay fractions are similar with respect to the limited number of parametric measurements, and a representative sub-sample (e.g.; a 25-50 sample suite depending measurement cost, time demand, and importance) of the characterized sediments will be subjected to more detailed second-tier measurements to further define and bound key geochemical parameters that control U(VI) solid-liquid distribution and kinetic response. The identity of these key parameters will be further refined through intact core and deconstructive experiments that will soon be initiated at both PNNL and USGS. The parameters described below represent current thinking; they may change as new information is developed on IFRC site sediments. A third-tier of characterization measurements that are not described here will define fundamental geochemical reaction and physical transport parameters needed to model the reactive transport behavior of U(VI) in the IFRC system.

A wet-sieving method will be used to complement particle size measurements performed by dry sieving during sample processing. The hydrometer method or laser diffraction spectrometry (LDS) will be used to determine the size distribution of the silt-clay fractions. The silt and clay size fractions will be separated using Stokes law settling velocities to determine the weight percentage of each size-fraction. The silt and clay size fractions of each sample will be saved for further mineralogical analysis as needed, using x-ray diffraction (XRD).

The Brunauer Emmett Teller (BET) surface area will be determined on the < 2 mm fraction by analysis of N₂ gas (or Kr if surface areas are < 1 m²/g) adsorption on 3 g samples. The samples will be outgassed for a minimum of 5 hours at 110°C and at 3 μm Hg pressure. The specific surface area will be measured at liquid nitrogen temperature (approximately 77 K) to allow N₂ adsorption at the solid surface. Surface area will also be measured on silt-clay fraction subsamples from the < 2mm samples studied to develop a correlation between silt-clay content of the <2 mm fraction and its surface area.

X-ray powder diffraction analysis of the individual silt-clay and sand fractions will be used to determine semi-quantitative mineral distributions (e.g., mass %), and their heterogeneity across the site. Magnesium, K, and ethylene glycol saturations will be applied to silt and clay to facilitate phyllosilicate identification (Zachara et al., 2002; Qafoku et al., 2005). Optical microscopy of the sand fraction will be applied to determine the mass distribution of prominent clast types including basalt, granite, and other; and the extent of particle coatings by fine grained materials (Stubbs et al., 2008).

Isotopic exchange using ²³³U and time variable bicarbonate extractions as described by Kohler et al., (2004), Bond et al., (2008), and Stoller et al., (2008) will be used to provide

insights on the distribution of U(VI) in IFRC samples displaying a range in total contaminant U(VI) as measured during initial characterization. The measurements will operationally discriminate between surface (adsorbed and freshly precipitated) and intragrain U (e.g., within the interior of rock fragments) providing information necessary to interpret the magnitude of kinetic and mass transfer behaviors when observed.

Alkalinity will be measured using a standard acid titration method. The alkalinity procedure is equivalent to the U.S. Geological survey method in the *National Field Manual for the Collection of Water-Quality Data* (USGS, 2004).

The total carbon concentration total organic carbon analyzer by combustion. Aliquots of sediment will be placed into pre-combusted, pre-weighed ceramic sample holders and weighed on a calibrated balance. After sparging, the sample will be combusted, and carbon quantitated using a non-dispersive infrared (NDIR) gas analyzer against calcium carbonate standards. Inorganic carbon will be determined in an analogous method with the addition of phosphoric acid at lower temperature, and organic carbon will be determined by difference between total and inorganic measurements.

Cation exchange capacity (CEC) will be determined by base saturation of the < 2 mm fraction with an index cation/chloride solution, displacement by ammonium chloride, and subsequent ICP-OES analyses. CEC is a needed parameter to describe groundwater composition buffering and changes that may result from river water infiltration or intentional injection of waters from different locations in the 300 A plume. Methodologies described in Zachara et al. (2002) and McKinley et al. (2007) will be adapted for application to 300 A sediments.

Multiple reagent Fe extractions will be used to target amorphous versus more crystalline iron-oxide phases (Anderson and Jenne, 1970; Dong et al., 2005; Loeppert and Inskeep, 1996; McAlister and Smith, 1999). Hydroxylamine hydrochloride (HH) in nitric acid or ammonium oxalate with oxalic acid at pH 3 (AAO), will be used to extract only the amorphous iron oxides such as ferrihydrite (Chao and Zhou, 1983; Loeppert and Inskeep, 1996). A mixed solution of sodium citrate, sodium bicarbonate, and sodium dithionite (CBD) as described in (Loeppert and Inskeep, 1996), will be used to reductively extract crystalline Fe oxides. The extraction solutions will be filtered and analyzed for Fe, Mn, Al, and Si using ICP-OES.

Stirred-flow cell experiments (Liu et al., 2008) will be used to assess the extent and rates of mass transfer processes of non-reactive tracers and U(VI) in < 2 mm sediments of variable texture, U concentration, and mineralogy. This methodology is currently under development using newly retrieved sediments from the IFRC well field and a specially designed flow cell. The applicability of these measurements to “field scale” processes will be evaluated as part of the intact core and deconstructive experiment series.

Table 5-2. Composition of 300 Area groundwaters collected from various excavations in February through April, 2003.

	618-5 Pit 1 (26 Feb 03)	618-5 Pit 1 (29 May 03)	618-5 Pit 2 (26 Feb 03)	SPP Pit 1 (19 Apr 03)	SPP Pit 2 (19 Apr 03)	NPP Pit 1 (26 Apr 03)	NPP Pit 2 (26 Apr 03)	Range
pH	7.71	8.11	7.80	7.83	8.04	7.83	7.88	7.71 - 8.11
Ionic Strength (mmol/L)	7.5	8.2	7.5	3.5	4.9	5.2	6.3	3.5 - 8.2
<u>Cations</u> (mmol/L)								
Ca	1.31	1.17	1.24	0.60	0.90	1.01	1.14	0.60 - 1.31
K	0.16	0.20	0.16	0.07	0.09	0.07	0.06	0.06 - 0.20
Mg	0.58	0.49	0.56	0.21	0.28	0.34	0.40	0.21 - 0.58
Na	1.34	2.65	1.53	0.77	0.95	0.84	1.14	0.77 - 2.65
<u>Anions</u> (mmol/L)								
Cl ⁻	0.84	1.21	0.76	0.14	0.36	0.36	0.39	0.14 - 1.21
NO ₃ ⁻	0.42	0.53	0.40	0.36	0.40	0.29	0.43	0.29 - 0.53
Inorg. C	2.47	2.71	2.41	1.20	1.70	2.02	1.58	1.20 - 2.71
SO ₄ ²⁻	0.69	0.76	0.85	0.35	0.43	0.47	0.88	0.35 - 0.88
Si _{Total}	0.57	0.59	0.55	0.28	0.39	0.32	0.23	0.23 - 0.59
<u>U (μmol/L)</u>								
Species (%)	(%)	(%)	(%)	(%)	(%)	(%)	(%)	
UO ₂ (CO ₃) ₂ ²⁻	5.8	2.8	5.4	22.0	6.2	7.1	7.3	0.30 - 4.96
UO ₂ (CO ₃) ₃ ⁴⁻	3.5	5.0	4.0	6.5	4.7	4.0	3.9	
Ca ₂ UO ₂ (CO ₃) ₃ ⁰	90.6	92.2	90.5	70.4	88.9	88.7	88.6	
P _{CO2}	-2.559	-2.912	-2.656	-2.971	-3.035	-2.754	-2.913	

5.6 Hydrologic Characterization

Laboratory hydrologic characterization will primarily consist of measurements of saturated hydraulic conductivity and relative permeability-saturation-capillary pressure (k-S-P) relations on approximately 40 intact or composite sediment samples. However, as noted in Section 5.4.7, many properties such as electrical resistivity, thermal conductivity and heat capacity are saturation-dependent. Therefore measurements of these properties as a function of water saturation will also be made simultaneously on selected samples. Additional measurements of saturated hydraulic conductivity will also be performed on repacked sediments using a custom-developed apparatus designed specifically for very coarse sediments, as described below.

5.6.1 Saturated Hydraulic Conductivity

Saturated hydraulic conductivity will be measured on undisturbed cores and repacked sediment mixtures using both the constant and falling head methods (Reynolds and Elrick, 2002). The constant head method is usually preferable for coarse, high permeability sediments while the falling head method is typically used for sediments of relatively low to moderate permeability. Although the Hanford formation sediments are generally quite coarse with very high hydraulic conductivities (>1000 m/d), the underlying Ringold Formation sediments can be relatively fine-grained and typically have hydraulic conductivities that roughly two-orders-of-magnitude lower than the Hanford formation sediments. Therefore we will use whichever hydraulic conductivity measurement method is best suited for the particular samples that are being analyzed.

Saturated hydraulic conductivity (K_s) is a critical hydraulic property needed to characterize heterogeneous sediments, and its prediction from grain-size distributions has been the subject of numerous studies. Measurements of K_s as function of grain size and sorting will improve our understanding of the relationship between grain-size distribution and hydraulic conductivity and support development of a robust method for quantifying the effect of gravel on hydraulic conductivity estimates. Hydraulic conductivity measurements of repacked grab samples will be performed in large permeameters, designed such that the sample holder is approximately 8 or 12 times the maximum particle size of the sediment to be characterized (ASTM 2006b). **Figure 5-5** shows photograph of the 4-in.-diameter permeameter, which is based on a design described in a soil mechanics note by the USDA Soil Conservation Service (USDA 1984). An 8-in model is also available for coarser materials.

To measure K_s , enough of the sample is weighed out to pack the permeameter to a height of 15 cm at the desired density. The material will be packed so as to avoid segregation during emplacement and to reflect the observed field densities. The permeameter will then be vibrated to obtain the required packing density. The permeameter will then be connected to a water supply, and water will be allowed to flow upward through the sample at the desired rate until flow becomes steady. The volumetric flow rate, Q , passing through the cross sectional area, A , of the permeameter is recorded as a function of time, t . The hydraulic head gradient ($i=\Delta h/L$) will also be determined from the piezometers installed at the top and bottom (separated by distance L) of the permeameter. For each sample, the hydraulic-head gradient is plotted against the Darcy velocity ($v=Q/A$), and K_s is determined from the slope of the line. These measurements will be repeated for various sediment size separates, model binary mixtures, and the end members of the binary mixtures at several flow rates. This information is needed to allow correction of K_s estimates for the presence of gravel.

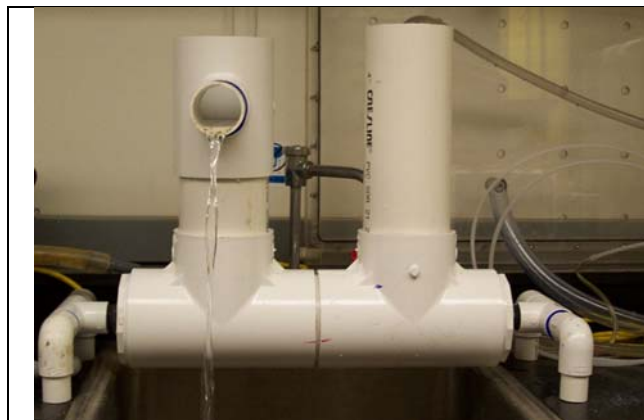


Figure 5-5. Photograph of the 4-inch-diameter permeameter used to measure hydraulic conductivity of coarse sands and gravel.

An apparatus for falling head hydraulic conductivity measurements is depicted in **Figure 5-6**. Each core liner will be first fitted with two machined plexiglas® collars, one at each end, to allow attachment of end plates. After attaching the end plates, the core will be saturated and weighed, and a small-diameter reservoir attached to one end of the sample. A burette was used as the small-diameter reservoir for the demonstrated measurements. The burette will be filled with water and the height at time zero, h_0 , recorded.

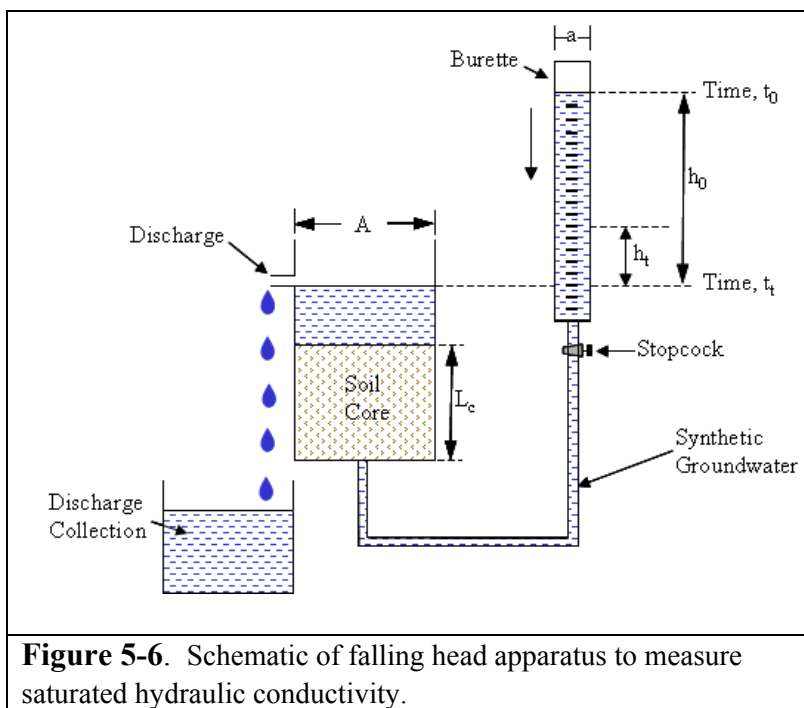


Figure 5-6. Schematic of falling head apparatus to measure saturated hydraulic conductivity.

The measurement is started by opening the burette stopcock and the rate of decline of the water level in the burette is recorded over time. The hydraulic head at the upgradient end of the sample is allowed to decline from h_0 , at time 0 (t_0), to h_t at some time t (t_t). Calculation of K_s is based on Darcy's Law, with K_s being defined as:

$$K_s = \left(\frac{d_r}{d_c} \right)^2 \cdot \left[\frac{L_c}{t_t - t_0} \right] \cdot \log \left(\frac{h_0}{h_t} \right)$$

where d_r is the diameter of the reservoir, L_c is the length of the core sample, and d_c is the

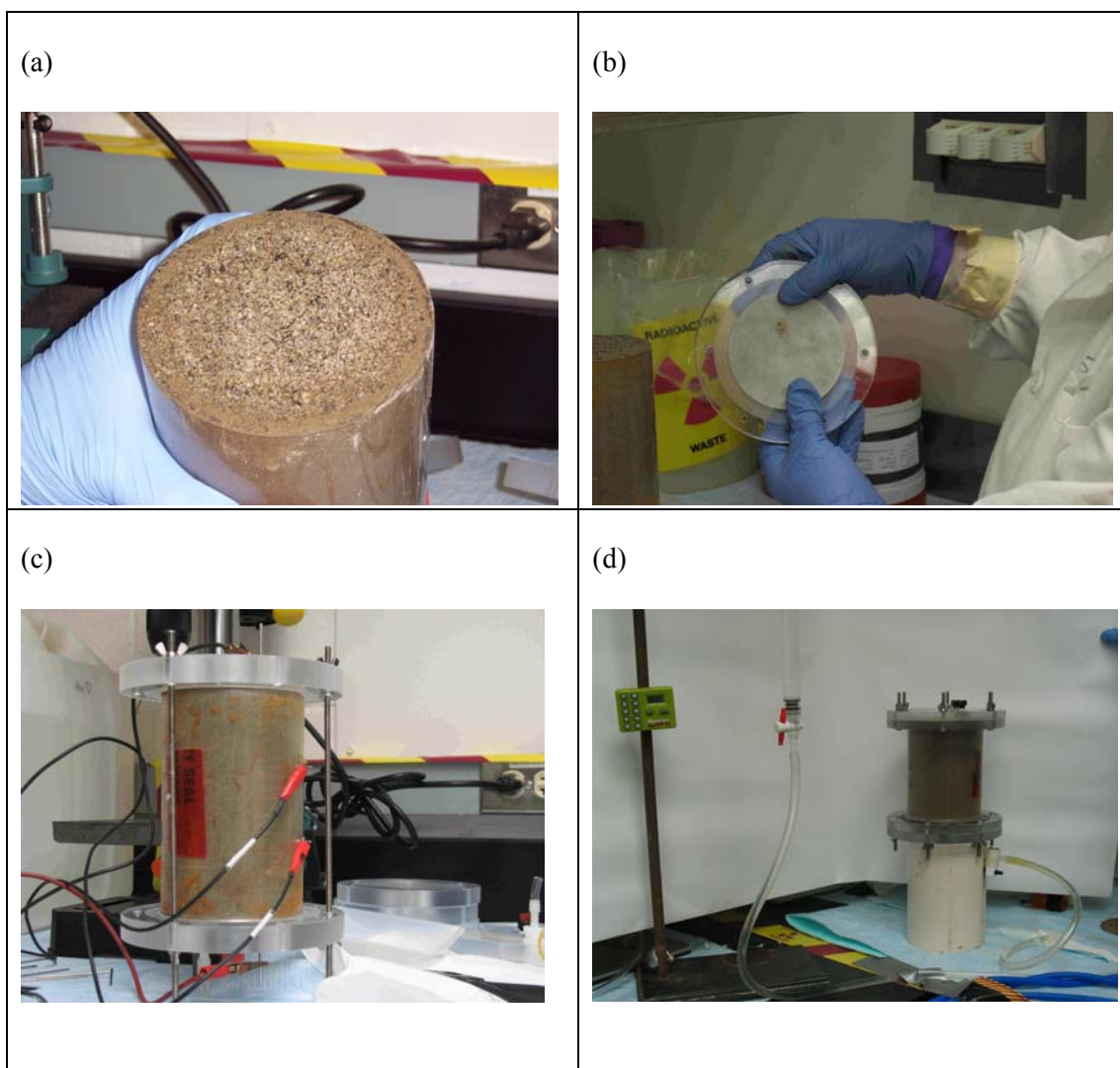


Figure 5-7. Stages of core preparation for falling head conductivity measurements, (a) soil core just after removal of end caps, (b) porous stainless steel electrode in the end cap used for unsaturated hydraulic and electrical measurements, (c) fully assembled core with collars and end caps and electrodes for electrical measurements, and (d) falling head apparatus for measuring saturated hydraulic conductivity.

diameter of the core. Each measurement will be repeated three times using different initial hydraulic gradients and the mean K_s will be calculated. For very coarse samples, it can be difficult to visually measure the rate of drop of water in the burette. However, by using a pressure transducer and datalogger, the water level in the burette can be automatically measured as a function of time so that direct visual observation and manual recording of water levels is not required. **Figure 5-7** shows different stages of core preparation for saturated hydraulic conductivity measurements and the soaking tank with fixed overflow used for containing the permeability cell during a falling head test.

Measurements of relative permeability-saturation-capillary pressure (k-S-p) relations will also be made on ~40 samples (on which K_s measurements were also made) using the multi-step outflow method (Dane and Topp, 2002) with an automated measurement system (**Figure 5-8**) housed in EMSL's Subsurface Flow and Transport Experimental Laboratory (SFTEL). Larger diameter columns and end plates for the apparatus depicted in **Figure 5-8** will be machined, as necessary, to accommodate very coarse samples. The bulk and particle densities and porosities of the cores on which these K_s and k-S-P measurements are made will also be determined.

The K_s , k-S-p, density, and porosity data described above, and U(VI) adsorption data determined on these and other samples for which detailed grain-size distribution data are also available, will be used to develop hydraulic property and adsorption isotherm scaling relationships (Rockhold et al., 1996; Snyder, 1996; Böttcher 1997). These data will also be used in conjunction with grain-size distribution data to generate so-called pedotransfer functions that relate measured hydraulic and sorption properties to key grain-size distribution metrics (Ward et al. 2006; Guber et al. 2006). These scaling relationships and pedotransfer functions will be applicable to estimation of hydraulic and adsorption parameters based on direct measurements of grain-size distributions and their metrics determined on core or bucket samples, as well as from indirect measurements based on geophysical well logging data (e.g. spectral gamma logs; K-40 or total gamma), and/or cross-well characterization methods.



Figure 5-8. Apparatus for automated, laboratory measurement of sediment hydraulic properties (k-S-p relations) in EMSL (SFTEL).

6.0 Data Integration

All characterization data develop through these measurements and study will be input to the password protected, Hanford IFRC data base that is accessible through the web-site. This data base is accessible to IFRC project participants and ERSD management. The data is subject to courtesy and use restrictions, as specified in the data base and as discussed in IFRC management communications, to protect data steward rights. Data integration will formally occur through mathematical manipulation using the UCB – MAD software; and inverse, hydrologic, and reactive transport modeling of different types that will be described in a subsequent Hanford IFRC Modeling Plan.

7.0 Characterization Summary

A variety of field and laboratory measurements are planned for the IFRC experimental site that are summarized in **Table 7-1**. These measurements support the development of a geostatistical model of the IFRC site that includes the spatial variance of lithofacies, hydraulic conductivity, porosity, contaminant U(VI) distribution, sorbent concentrations and surface complexation parameters, mass transfer rates, and other relevant properties. The characterization data is intended, among other uses, to: i.) populate reactive transport models for experiment interpretation, ii.) support correlations of different sort between intensive and extensive parameters, and iii.) provide basis for interpolation of subsurface properties between wells at different depths. The characterization data will also support mechanistic, process-focused experimentation on selected subsets of subsurface materials from the site. Modifications to this plan will likely occur as results accumulate.

Table 7-1. Summary of baseline characterization measurements for IFRC well field.

Report Section	Measurement Subject	Measurement Type	Characterization Info.	Measurement Frequency and/or Number
2.1	Borehole with temporary casing	Neutron moisture	Water content	Twenty-nine (of 35) wells at 7.5 cm resolution in vadose zone
2.1	Borehole with temporary casing	γ -ray spectroscopy	Lithology	Twenty-nine (of 35) wells at 15 cm resolution
2.2	4" PVC well	Density probe	Bulk density	All wells with approximate 10 cm resolution
2.2	4" PVC well	Neutron porosity	Bulk density	All wells with approximate 10 cm resolution
2.2	4" PVC well	Electrical conductivity and magnetic susceptibility	Integrates multiple effects; sensitive to porosity, saturation, dissolved salts, and temperature	All wells with 0.5 m resolution
2.2	4" PVC well	Borehole inclination	Inclination, bearing, true depth	All wells
2.2	4" PVC well	Acoustic tele-viewer	Acoustic information on region near the well casing, fractures, voids, etc.	All wells with ~ 3 cm resolution
2.2	4" PVC well	Neutron moisture	Changing water content in vadose zone	All wells with ~ 10 cm resolution in vadose zone
2.2	4" PVC well	Borehole radar with single off-set borehole surveys; more comprehensive measurements later	Orientation and thickness of dissimilar units	All wells with ~ 0.2 m resolution in saturated zone
2.2	4" PVC well with ERT electrode strings	Crosshole resistivity	Electrical properties related to lithology, water content, and salt content	28 instrumented resistivity wells containing 840 electrodes
3.0	4" PVC well	Opportunity pumped groundwater samples	Dissolved concentrations of major and minor ions and	Pumped samples from all wells at low, high, and two intermediate river

			U(VI)	stages (e.g., Sept., Jan., April, July)
3.0	4" PVC well	Passive, multi-level sampler	Vertical groundwater composition	Four wells during stable periods of low and high river stage
3.0	4" PVC well	Smear zone samples	Water composition at water table	Time-series for six wells at rising and declining river stage (spring/summer 09)
4.2	4" PVC wells/saturated zone	Electromagnetic borehole flowmeter	Vertical distribution of horizontal hydraulic conductivity	All wells. Temporal measurements performed in 10 wells
4.2	4" PVC wells/saturated zone	Constant rate injection test	Quantitative hydraulic property estimates	Multiple; methodology and injection volume needs and rates under assessment
4.3	4" PVC wells	Non-reactive tracer experiment w ~ 100,000 gal of 80 ppm NaBr in IFRC well water	Assess heterogeneities and transport velocities in the saturated zone; test well-field infrastructure	One experiment planned for Dec. 2008
5.4	Borehole sediments	Particle size distribution	Distribution of gravel, sand, silt, and clay; and subclasses	100 grab and 25 core samples
5.4	Borehole sediments	Hele-Shaw cell	Particle shape	25 separate size fractions
5.4	Borehole sediments	Porosity on loose and dense packs	Data for packing model	25 grab samples
5.4	Borehole sediments	Pycnometer	Particle density	25 < 2 mm size fractions
5.4	Borehole sediments	Single point, N ₂ adsorption	Surface area	25, < 2 mm size fractions of grab samples
5.4	Borehole sediments	Impedance spectroscopy as a function of saturation	Sediment electrical properties	50 intact cores
5.4	Borehole sediments	Electrical resistivity and induced polarization as a function of saturation	Sediment electrical properties	25 intact cores
5.4	Borehole sediments	Thermal properties as a function of saturation	Sediment heat capacity and diffusivity	25 intact cores

5.4	Borehole sediments	γ spectroscopy measurements of ^{40}K , ^{238}U , ^{232}Th	Isotopic signatures for interpretation of SGLS	25 samples of gravel, sand, silt, and clay
5.5	Borehole sediments	Fusion and digestion	Total and contaminant U	200 grab samples
5.5	Borehole sediments	2 week bicarbonate extraction	Labile adsorbed U(VI)	200 grab samples
5.5	Borehole sediments	Acidified hydroxyl amine hydrochloride (AHH)	Reactive Al and Fe oxides	200 grab samples
5.5	Borehole sediments	Single point K_d measurements at 60 $\mu\text{g/L}$ U(VI)	Linkage to surface complexation model	200 grab samples in two synthetic groundwaters representative of high and low river stage
5.5	Borehole sediments	X-ray diffraction	Mineral distribution	25 samples(each) of sand, silt, and clay from the saturated zone
5.5	Borehole sediments	Isotopic exchange	Labile adsorbed U(VI) and precipitated U(VI)	25, < 2 mm samples that vary in total U(VI)
5.5	Borehole sediments	Total carbon by combustion	Sediment inorganic and organic carbon	A total of 50 vadose and saturated zone sediments
5.5	Borehole sediments	Cation exchange capacity	Fixed negative charge on sediment particles	25, < 2 mm separates of saturated zone sediments
5.5	Borehole sediments	AAO and CBD extractions for Fe(III)	Amorphous and crystalline Fe(III) oxides	25, < 2 mm separates of saturated zone sediments
5.5	Borehole sediments	Stirred flow reactor adsorption/desorption experiments with 60 $\mu\text{g/L}$ U(VI) in 300A SGW-1 and 300A SGW-2.	Grain-scale mass transfer rates	25, < 2 mm separates of saturated zone sediments
5.6	Borehole sediments	Constant and falling head methods	Saturated hydraulic conductivity (K_s)	40 intact cores and 40 repacked grab samples
5.6	Borehole sediments	Multistep outflow method	Relative permeability – saturation – capillary pressure relations	40 samples on which K_s measurements were performed

8.0 References

- Anderson, B. J., and Jenne, E. A.. 1970. Free-iron and manganese oxide content of reference clays. *Soil Sci.*, **109**:163-169.
- ASTM_D422_86. 1986. Standard Test Method for Particle Size Analysis of Soils, Annual Book of ASTM Standards. American Society of Testing Material, Philadelphia, PA.
- ASTM_D854-06. 2006. Standard Test Methods for Specific Gravity of Soil Solids by Water Pycnometer, Annual Book of ASTM Standards. American Society of Testing Material, Philadelphia, PA.
- ASTM_D2216-98. 1986. Laboratory Determination of Water (Moisture) Content of Soil, Rock, and Soil-Aggregate Mixtures, Annual Book of ASTM Standards. American Society of Testing Material, Philadelphia, PA.
- ASTM_E1915-01. 2001. Standard Test Methods for Analysis of Metal Bearing Ores and Related Materials by Combustion Infrared Absorption Spectrometry, Annual Book of ASTM Standards. American Society of Testing Material, Philadelphia, PA.
- American Society of Testing and Materials (ASTM). 2006a. Standard Test Method for Particle-Size Analysis of Soils. *ASTM D422-63*, Philadelphia, Pennsylvania.
- American Society of Testing and Materials (ASTM). 2006b. Standard Test Method for Permeability of Granular Soils (Constant Head). *ASTM D2434-68*, Philadelphia, Pennsylvania.
- Bjornstad, B. N. and Horner, J. 2008. Drilling, Sampling, and Well-Installation Plan for the IFRC Well Field, 300 Area. *PNNL-17512*, Pacific Northwest National Laboratory, Richland, WA.
- Bjornstad, B. N. and Vermeul, V. R. 2008. Drilling Specifications: Well Installations in the 300 Area to Support PNNL's Integrated Field-Scale Subsurface Research Challenge (IFRC) Project. *PNNL-17199*, Pacific Northwest National Laboratory, Richland, WA.
- Blake, G. R., and Hartge, K. H. 1986. Particle Density. In: *Methods of Soil Analysis, Part 1, Physical and Mineralogical Methods*. A. Klute (ed.), pp. 377–382, American Society of Agronomy, Madison, WI.
- Bond, D. L., Davis, J. A., and Zachara J. M. 2007. Uranium(VI) release from contaminated vadose zone sediments: estimation of potential contributions from dissolution and desorption. In: *Adsorption of Metals by Geomedia II* (M. O. Barnett and D. B. Kent, eds.), pp. 379-420. Academic Press, San Diego, CA.
- Böttcher, J. 1997. Use of scaling to quantify variability of heavy metal sorption isotherms. *Euro. J. Soil Sci.* **48**:379-386.

- Briesmeister, J. F. 1997. MCNP- A Aeneral Monte Carlo N-Particle Transport Code, Version 4B. *LA-12625-M*, Los Alamos National Laboratory, Los Alamos, NM.
- Brunauer, S., Emmet, P. H., and Teller, E. 1938. Adsorption of gases in multimolecular layers. *J. Am. Chem. Soc.*, **60**:309-319.
- Chao, T. T. and Zhou, L. 1983. Extraction techniques for selective dissolution of amorphous iron oxides from soils and sediments. *Soil Sci. Soc. Am. J.*, **47**:225-232.
- Coston, J. A., Fuller, C. C., and Davis, J. A. 1995. Pb²⁺ and Zn²⁺ adsorption by natural aluminum- and iron-bearing surface coating on an aquifer sand. *Geochim. Cosmochim. Acta* **59**(17):3535-3547.
- Curtis, G. P., Fox, P., Kohler, M. and Davis, J. A. 2004. Comparison of in situ uranium K_d values with a laboratory determined surface complexation model. *Appl. Geochem.*, **19**:1643-1653.
- Dagan G. 1989. *Flow and Transport in Porous Formations*. Springer-Verlag, Berlin, Germany.
- Dane, J. H., and Topp, G. C. 2002. Methods of soil analysis, Part 4. In: *Physical Methods*, Soil Science Society of America.
- Davis, J. A., and Curtis, G. P. 2003. Application of Surface Complexation Modeling to Describe Uranium(VI) Adsorption and Retardation at the Uranium Mill Tailings Site at Naturita, Colorado. *NUREG CR-6820*, U.S. Nuclear Regulatory Commission, Rockville, MD.
- Dong, W., Ball, W. P., Liu, C., Wang, Z., Stone, A. T., Bai, J. and Zachara, J. M. 2005. Influence of calcite and dissolved calcium on uranium(VI) sorption to a Hanford subsurface sediment. *Environ. Sci. Technol.*, **39**:7949-7955.
- Engelman, R. E., Lewis, R. E., Stromswold, D. C., and Hearst, J. R. 1995. Calibration Models for Measuring Moisture in Unsaturated Formations by Neutron Logging. *PNL-10801*, Pacific Northwest National Laboratory, Richland, WA.
- EPA_Method_6020. 2000. Inductively Coupled Plasma-Mass Spectrometry, Test Methods for Evaluating Solid Waste, Physical/Chemical Methods. *EPA Publication SW-846*, available online <http://www.epa.gov/epaoswer/hazwaste/test/sw846.htm>.
- Fienen, M. N., Kitanidis, P. K., Watson, D., and Jardine, P. 2004. An application of Bayesian inverse methods to vertical deconvolution of hydraulic conductivity in a heterogeneous aquifer at Oak Ridge National Laboratory. *Mathematical Geol.*, **36**(1):101-126.

- Finkel, M., and Liedl, R. 1998. Retarded intraparticle diffusion in heterogeneous aquifer material. In: *Water–Rock Interaction*, G. B. Arehart and J. R. Hulston (Eds). Balkema, Rotterdam, pp. 219–222.
- Friedman, S. P., and Robinson, D. A. 2002. Particle shape characterization using angle of repose measurements for predicting the effective permittivity and electrical conductivity of saturated granular media. *Water Resour. Res.* **38**(11):0043–1397.
- Gelhar, L. W. 1993. *Stochastic Subsurface Hydrology*. Prentice-Hall, Englewood Cliffs, NJ.
- Grathwohl, P. and Kleineidam, S. 1995. Organic Contaminants. In: *Groundwater Quality: Remediation and Protection*, K. K. Krasny (Eds). IAHS Publ. **225**:79–86.
- Guber, A. K., Pachepsky, Y. A., van Genuchten, M. Th., Rawls, W. J., Simunek, J., Jacques, D., Nicholson, T. J., and Cady, R. E. 2006. Field-scale water flow simulations using ensembles of pedotransfer functions for soil water retention. *Vadose Zone J.* **5**:234–247.
- Keller, J., Ward, A. L., Schenter, R. E., and Wittman, R. S. 2005. The effect of layered heterogeneity on the response of neutron moisture probes. Soil Science Society of America Annual Meeting, Salt Lake City, UT.
<http://crops.confex.com/crops/2005am/techprogram/P8429.HTM>
- Kogan, R. M., Nazarov, I. M., and Fridman, Sh. D. 1969. Gamma Spectrometry of Natural Environments and Formations. Environmental Science Services Administration, U.S. Department of Commerce and the National Science Foundation, Washington, D.C.
- Kohler, M., Curtis, G. P., Meece, D. E., and Davis, J. A. 2004. Methods for estimating adsorbed uranium(VI) and distribution coefficients of contaminated sediments. *Environ. Sci. Technol.*, **38**:240-247.
- Li, J., Smith, D. W., Fityus, S. G., and Sheng, D. 2003. Numerical analysis of neutron moisture probe measurements. *Int. J. Geomechanics*, **3**(1):11-20.
- Li, W., Englert, A., Cirpka, O. A., and Vereecken, H. 2008. Three-dimensional geostatistical inversion of flowmeter and pumping test data. *Groundwater* **46**(2):193-201.
- Lockner, D. A., and Byerlee, J. D. 1985. Complex resistivity measurements of confined rock. *J. Geophys. Res.*, **90**:7837-7847.
- Loeppert, R. H., and Inskeep, W. P. 1996. Iron. In: *Methods of Soil Analysis, Part 3-Chemical Methods*; Sparks, D. L. (Ed.). Soil Science Society of America, Inc., pp. 639-664, Madison, WI.

- Macdonald, J. R. 1985. Generalizations of "universal dielectric response" and a general distribution-of-activation-energies model for dielectric and conducting systems. *J. Appl. Phys.*, **58**:1971-1978.
- McAlister, J. J., and Smith, B. J. 1999. Selectivity of ammonium acetate, hydroxylamine hydrochloride, and oxalic ascorbic acid solutions for the speciation of Fe, Mn, Zn, Cu, Ni, and Al in early tertiary paleosols. *Microchem. Journal*, **63**:415-426.
- McKinley, J. P., Zachara, J. M., Smith, S. C., and Liu, C. 2007. Cation exchange reactions controlling desorption of $^{90}\text{Sr}^{2+}$ from coarse-grained contaminated sediments at the Hanford formation, Washington. *Geochim. Cosmochim. Acta* **71**: 305-325.
- Mickael, M. W. 1991. A study of Monte Carlo modelling errors for neutron porosity instrument responses. *Nuclear Geophys.*, **5**(4):421-428.
- Nyhan, J. W., Martinez, J. L., and Langhorst, G. J. 1994. Calibration of Neutron Moisture Gauges and Their Ability to Spatially Determine Soil Water Content in Environmental Studies. *LA-12831-MS*, Los Alamos National Laboratory, Los Alamos, NM.
- Olhoeft, G. R. 1979. Electrical properties. In: *Initial Report of the Petrophysics Laboratory*, G. R. Hunt, G. R. Johnson, G. R. Olhoeft, D. E. Watson, and K. Watson (Eds.), *U.S. Geol. Surv. Circ.*, **789**:1-26.
- Olhoeft, G. R. 1985. Low frequency electrical properties. *Geophysics* **50**:2492-2503.
- Ochsner, T. E., Horton, R., and Ren, T. 2001. Simultaneous water content, air-filled porosity, and bulk density measurements with thermo-TDR. *Soil Sci. Soc. Am. J.* **65**:1618-1622.
- PNNL. 1990. Procedures for Groundwater Investigations. *PNL-MA-567-DO-1*, Pacific Northwest National Laboratory, Richland, WA.
- PNNL. 1997. Gamma Energy Analysis Operation and Instrument Verification Using the Genie2000TM Support Software. *PNNL-RRL-01*, Pacific Northwest National Laboratory, Richland, WA.
- Ptak, T., and Strobel, H. 1998. Sorption of fluorescent tracers in a physically and chemically heterogeneous aquifer material. In: *Water-Rock Interaction: Proceedings of the 9th International Symposium on Water-Rock Interaction, WRI-9*, G. B. Arehart and J. R. Hulston (Eds), pp. 177-180. March 30-April 3, 1998, Taupo, New Zealand. A.A. Balkema, Rotterdam, the Netherlands.
- Qafoku, N. P., Zachara, J. M., Liu, C., Gassman, P. L., Qafoku, O. S., and Smith, S. C. 2005. Kinetic desorption and sorption of U(VI) during reactive transport in a contaminated Hanford sediment. *Environ. Sci. Technol.*, **39**: 3157-3165.

- Ren, T., Ochsner, T. E., and Horton, R. 2003. Development of thermo-time domain reflectometry for vadose zone measurements. *Vadose Zone J.*, **2**:544–551.
- Reynolds, W. D., and Elrick, D. E. 2002. Constant head soil core (tank) method. In: *Methods of Soil Analysis* Dane, J. H. and G.C. Topp (Eds), Part 4 - Physical Methods.
- Roberts, J. J., and Lin, W. 1997. Electrical properties of partially saturated Topopah Spring tuff: Water distribution as a function of saturation. *Water Resour. Res.*, **33**:557–587.
- Rockhold, M. L., Rossi, R. E., and Hills, R. G. 1996. Application of similar media scaling and conditional simulation for modeling water flow and tritium transport at the Las Cruces Trench Site. *Water Resour. Res.* **32**:595-609.
- Silva, O., and Grifoll, J. 2007. A soil-water retention function that includes the hyper-dry region through the BET adsorption isotherm. *Water Resour. Res.*, **43**:W11420, doi:10.1029/2006WR005325
- Snyder, V. A. 1996. Statistical hydraulic conductivity models and scaling of capillary phenomena in porous media. *Soil Sci. Soc. Am. J.* **60**:771-774.
- Stromswold, D. C. 1994. Calibration Facilities at Hanford for Gamma-Ray and Fission-Neutron Well Logging. *PNL-9958*, Pacific Northwest National Laboratory, Richland, WA.
- U.S. Department of Agriculture (USDA). 1984. *Permeability of Selected Clean Sands and Gravels*. Soil Mechanics Note No.9. Available at: <http://www.info.usda.gov/CED/ftp/CED/smn09.pdf>. Accessed April 2008.
- USGS. 2004. Alkalinity and acid neutralizing capacity. In: *National Field Manual for the Collection of Water-Quality Data Rounds*, S. A. and F. D. Wilde (Eds). United States Geological Survey, Available online <http://water.usgs.gov/owq/fieldmanual/chapter6.6/html/section6.6.htm>.
- Ward, A. L., Conrda, M. E., Daily, W. D., Fink, J. B., Freedman, V. L., Gee, G. W., Hoverston, G. M., Keller, M. J., Majer, E. L., Murray, C. J., White, M. D., Yabusaki, S. B., and Zhang, Z. F. 2006. Vadose Aone Transport Field Study Summary Report. *PNNL-15443*. Pacific Northwest National Laboratory, Richland, WA.
- Weber, W. J., Jr., McGinley, P. M., and Katz, L. E. 1992. A distributed reactivity model for sorption by soils and sediments: 1. Conceptual basis and equilibrium assessments. *Environ. Sci. Technol.* **26**(10):1955–1962.
- Wentworth, C. K. 1922. A scale of grade and class terms for clastic sediments. *J. Geol.* **30**:377–392.
- Winfield, K. A., and Nimmo, J. R. 2002. Water retention and storage-Controlled liquid volume. In: *Methods of Soil Analysis, Part 4--Physical Methods*, J. H. Dane and G. C. Topp

(Eds). Soil Science Society of America Book Series No. 5: Madison, Wisconsin, Soil Science Society of America, p. 698-703.

Zachara, J. M., Smith, S. C., McKinley, J. P., Serne, R. J., and Gassman, P. L. 2002. Sorption of Cs^+ to micaceous subsurface sediments from the Hanford Site. *Geochim. Cosmochim. Acta* **66**(2):193-211.

Zachara, J. M., Brown, C., Christensen, J., Davis, J., Dresel, E., Kelly, S., McKinley, J., Serne, R. J., and Um, W. 2007. A Site-Wide Perspective on Uranium Geochemistry at the Hanford Site. *PNNL-17031*, Pacific Northwest National Laboratory, Richland, WA.

Vermeul, V. R., Williams, M. D., Fritz, B. G., Mackley, R. D., Mendoza, D. P., Newcomer, D. R., Rockhold, M. L., Williams, B. A., and Wellman, D. M. 2007. Treatability Test Plan for 300 Area Uranium Stabilization through Polyphosphate Injection. *PNNL-16571*, Pacific Northwest National Laboratory, Richland, WA.